

**SENIOR THESES**  
**DEPARTMENT OF PHYSICAL SCIENCES**  
**Morehead State University**

---

*Petrologic Classification of Igneous and Metamorphic Rocks* by  
Frank Baldrige

*X-Ray Analysis of Cave Sediments From Pigeon Water Cave of  
Northeastern Pine Mountain* by Billy B. Stapleton

*The Correlation of Stream-deposited Breccias In Bat Cave, Carter  
Caves, Kentucky* by James Bond

*Jointing and Faulting in Selected Areas of Eastern Kentucky* by  
Mark A. Blair

---

December 1993

<sup>o</sup>  
PETROLOGIC CLASSIFICATION OF IGNEOUS AND METAMORPHIC ROCKS

of northwestern North Carolina

*— all caps also*

---

A Research Paper

Presented to

the Department of Physical Sciences

Morehead State University

---

In Partial Fulfillment

of the Requirements for

Science 471

---

by

Frank Baldrige

December 1993

## TABLE OF CONTENTS

ABSTRACT.....	iii.
INTRODUCTION.....	1
TYPES OF METAMORPHISM.....	3
CLASSIFICATIONS OF IGNEOUS AND METAMORPHIC ROCKS.....	6
PROCEDURE FOR MAKING THIN SECTIONS.....	9
RESULTS.....	10
REFERENCES CITED.....	12

## TABLE OF FIGURES

FIGURE 1. Stratigraphic column.....	2
FIGURE 2. Contact metamorphism aureole.....	4
FIGURE 3. Depth and temperature increases.....	5
FIGURE 4. Schistosity with planar and linear texture.....	8

## PETROLOGIC CLASSIFICATION OF IGNEOUS AND METAMORPHIC ROCKS OF NORTHWESTERN NORTH CAROLINA.

BALDRIDGE, Frank M., Department of Physical Sciences, Morehead State University, Morehead, KY 40351

About 34 percent of the Earth's surface is made up of igneous and metamorphic rocks, the remaining 66 percent comes from weathered particles of igneous rocks that are later lithified into sedimentary layers. To classify igneous and metamorphic rocks the mineralogical characteristics and fabric must be determined. General observations can be made in the field but a thin section of the sample viewed with a polarizing microscope will produce more specific data.

Thin sections are actually thin slices of rock that are bonded to a glass slide and ground to a thickness of about 30 microns to enable them to transmit light. The effects of polarized light on each mineral is unique, therefore crystal structure can be determined. When mineral composition is used in conjunction with the rocks texture and microstructure the origin of the rock can be determined.

For this study field samples of igneous and metamorphic rocks were collected and the surrounding geology of the area was noted for later reference in determining metamorphic influences.

### CITED REFERENCES

Fisher, Pettijohn, Reed, Weaver, 1970, Studies of Appalachian Geology, John Wiley and Sons, pp. 195-271.

King, Philip B., Ferguson, Lawrence, Roberts, 1944, Geology and Manganese Deposits of Northeastern Tennessee, Division of Geology, State of Tennessee Department of Conservation.

Stuckey, Jasper L., Conrad, Stephen G., 1958, North Carolina. Division of Mineral Resources-Geologic Map of North Carolina

Winkler, Helmut G. F., 1974, Petrogenesis of Metamorphic Rocks, Springer, Verlag, New York, New York.

## INTRODUCTION

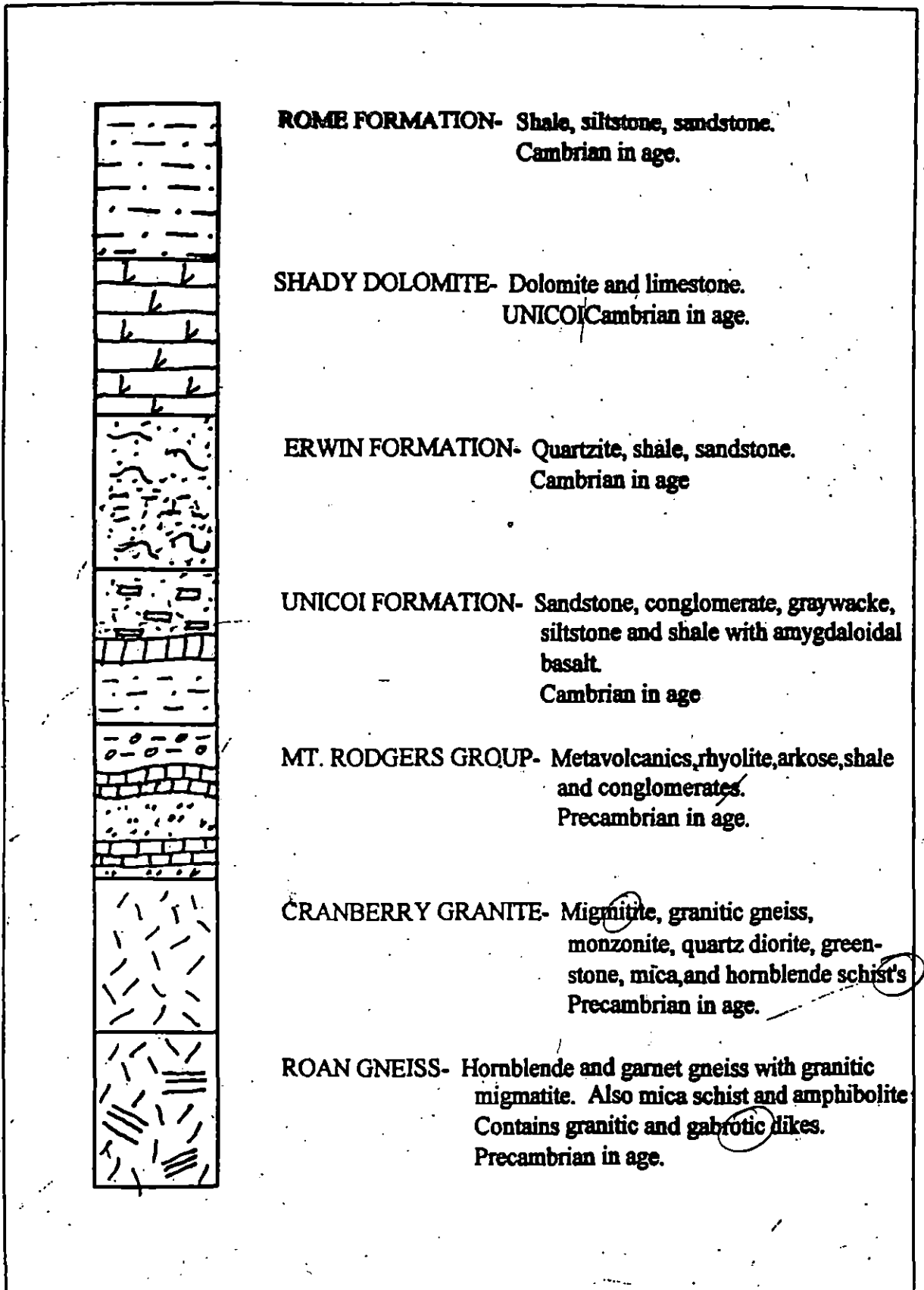
This study deals with igneous and metamorphic rocks collected from northwestern North Carolina in and around the Blue Ridge thrust sheet. Tectonic activity in the area has created a wide variety of metamorphic and igneous rock types; phyllite's, schist's, gneisse's, granite's, basalt's and gabbro's. Rocks range in age from cambrian to precambrian and are located within the stratigraphic section (Fig. 1). Thin sections were prepared to demonstrate texture and microstructure observable under a Petrographic microscope.

*perhaps  
not  
possibilities*

*What  
stratigraphic section?*

FIG. 1

## STRATIGRAPHIC SECTION



## TYPES OF METAMORPHISM

*spacing problem*

There are two types of metamorphism in a geologic setting, local and regional. Local metamorphism can be divided into two types; contact and cataclastic. Contact metamorphism occurs when an igneous intrusion raises the temperature of the surrounding country rock or protolith. When the temperature is increased an aureole of metamorphic rocks is produced around the intrusive body (Fig. 2). The second type of local metamorphism is called cataclastic metamorphism, this usually occurs near faults and overthrusts. The mechanical crushing and shearing ~~present~~ increases temperature due to friction and alters the rocks fabric.

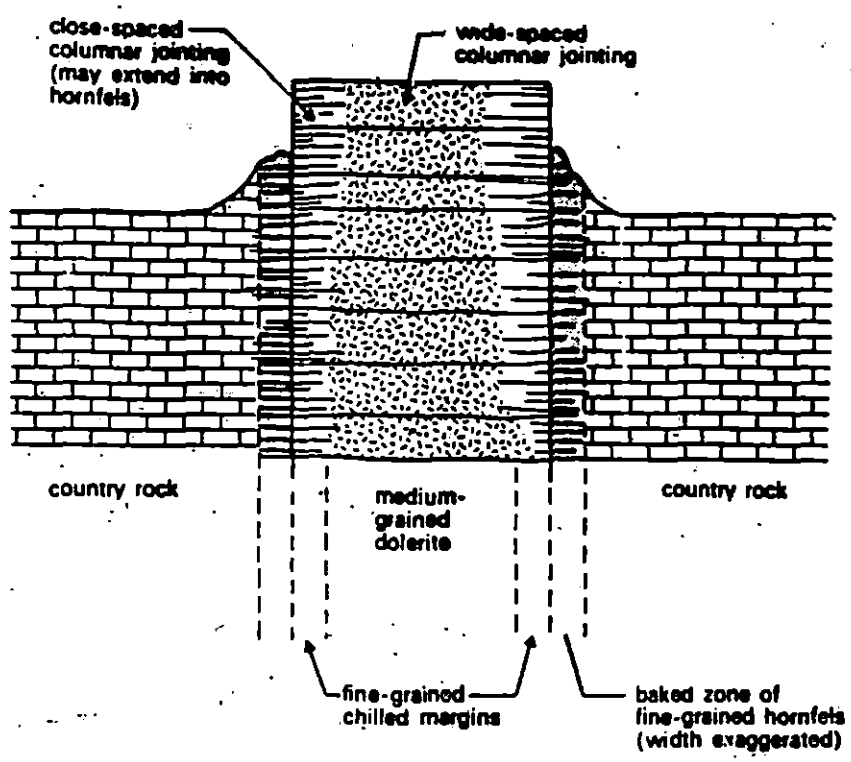
Regional metamorphism occurs in areas of larger proportions, usually hundreds to thousands of square kilometers in area. There are two types of regional metamorphism; regional dynamothermal and regional burial. Regional dynamothermal metamorphism is usually associated with large orogenic belts and is similar to contact metamorphism because alteration of the rock is due to a large supply of thermal energy which raises the steady state geothermal gradient to a high geothermal gradient which is hotter than the usual increase of 25 degrees centigrade per kilometer (Fig. 3).

Regional ~~Burial~~ metamorphism is not associated with orogenesis or magmatic intrusions and actually depends on burial of the section for an increase in temperature which follows the steady state geothermal gradient (Fig. 3 ). The maximum temperature obtained in burial metamorphism is usually around 400 to 500 degrees centigrade (Winkler, 1974).

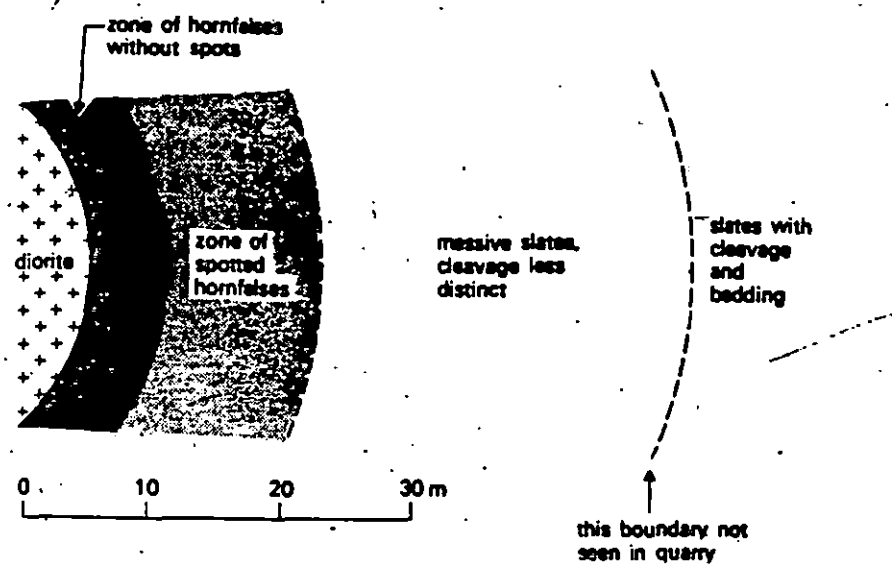


FIG. 2

CONTACT METAMORPHISM AUREOLE (FROM MASON, 1990)



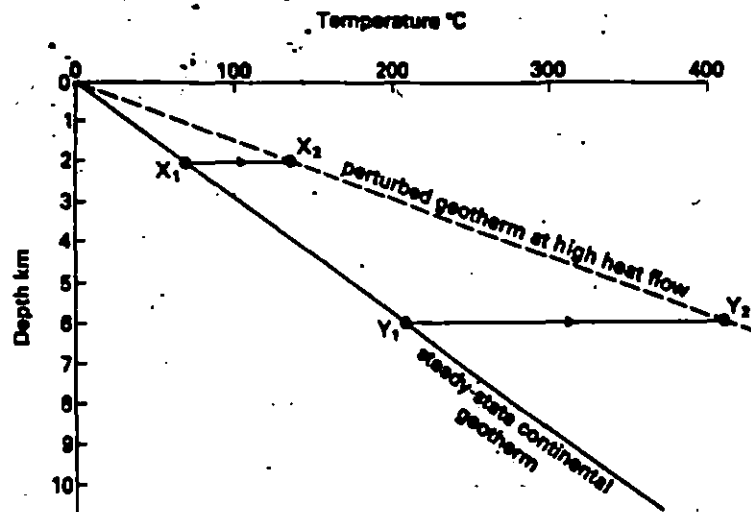
Cross section through a dolerite dyke 1 m wide, showing contact metamorphism of country rock.



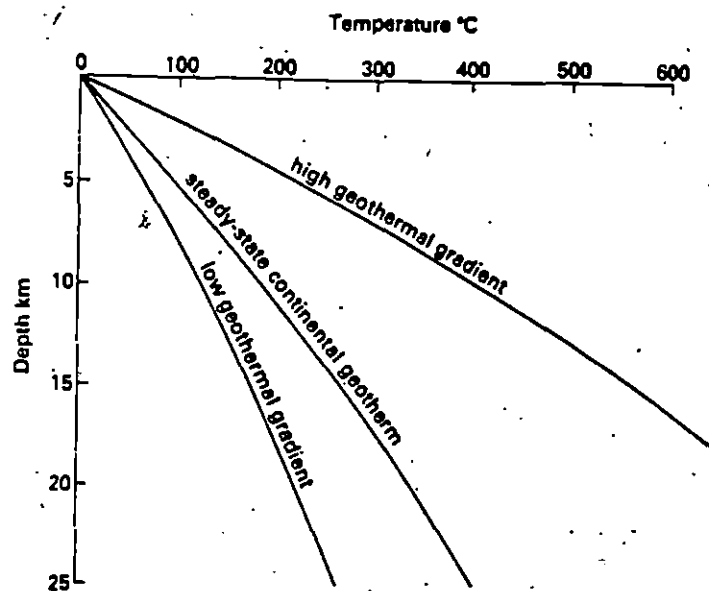
Schematic plan of the contact metamorphic zones seen in Cliffe Hill Quarry, Markfield, Leicestershire, England.

FIG. 3

## DEPTH AND TEMPERATURE INCREASES (FROM MASON, 1990)



Schematic geothermal gradients from example discussed in the text.  $X_1$ - $X_2$ , change in temperature of rock 2 km below surface,  $Y_1$ - $Y_2$ , change of temperature in rock 6 km below surface.



Depth-temperature curve for stable continental lithosphere, and for areas of high and low geothermal gradients.

## CLASSIFICATIONS OF IGNEOUS AND METAMORPHIC ROCKS

*Triple space below heading*

Igneous and metamorphic rocks are distinguished from each other by each rock's individual fabric. Igneous rocks are generally classified into three groups according to texture or crystal size; aphanitic, phaneritic and porphyritic. Aphanitic rocks are composed of small equal-sized crystals unable to be examined with the naked eye; they are generally formed when an igneous intrusion reaches the surface. The smaller crystal size is caused by the rapid cooling the rock undergoes <sup>or near</sup> at the surface. The second type of igneous rock is the phaneritic texture; it is composed of larger equal sized crystals which can be observed with the naked eye. Phaneritic rocks are formed when an igneous intrusion does not reach the surface and cools slowly allowing the crystals to grow larger. The third type of igneous rock is the porphyritic texture which has characteristics of aphanitic and phaneritic textures. Most of the rock is made up of an aphanitic texture but includes larger phenocrysts which are much larger than the surrounding groundmass which can be observed in a thin section of the rock. Porphyritic rocks are usually formed when an intrusion cools at depth allowing large crystals to form, then the intrusion reaches the surface where it cools quickly forming the smaller crystals that surround the larger ones (Ehlers, 1980).

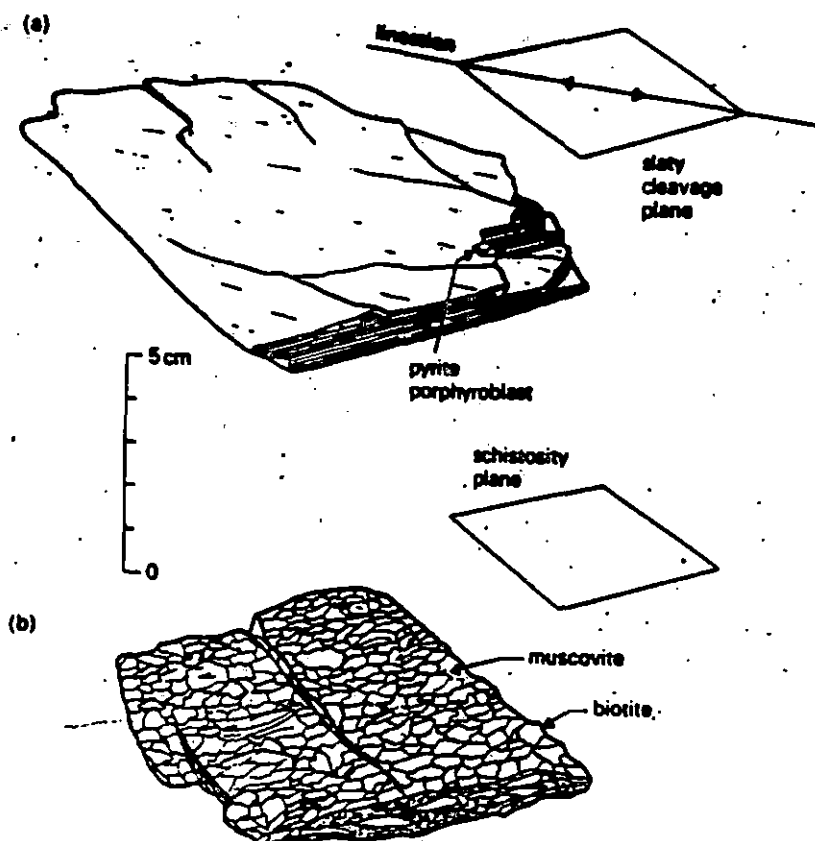
The classification of metamorphic rocks is extremely diverse due to differing types of metamorphism and mineral content so only the three types found in the field samples will be discussed; phyllites, schists and gneisses. Metamorphic rocks are

generally classified by individual grain size and the presence of schistosity which can be broken into two types linear and planar (Fig. 4). Phyllites are fine-grained and very finely schistose rock; the grain size is coarser than in slates but finer than in mica schists. Schists are medium to coarse-grained rock with an excellent parallelism of planar and or linear fabric which causes them to split into thinner plates than gneisses. Gneisses are medium to coarse-grained rock that splits into plates and angular blocks. Gneisses are also characterized by alternating light and dark bands formed from mineral grouping caused by the higher temperature and pressure this rock type forms under (Winkler, 1974).

Metamorphic rocks can be further classified by mineral composition determined in a thin section. For this study thin sections were made of each rock type but the equipment available would only produce usable thin sections of the higher grade metamorphic rocks, for this reason actual mineral composition of the field samples will not be discussed. However thin sections of the lower-grade metamorphic rocks were able to show the schistosity of the samples which will indicate the type of metamorphism the rocks were formed in.

FIG. 4

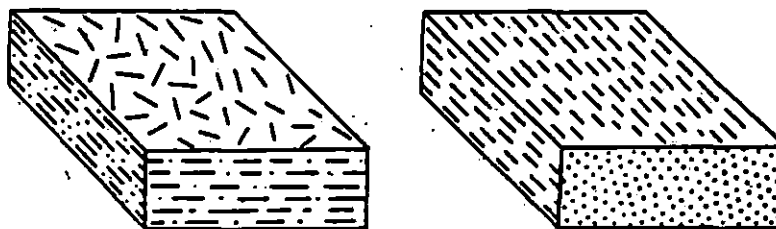
## SCHISTOSITY WITH PLANAR AND LINEAR TEXTURE (FROM MASON, 1990)



Hand specimens of (a) slate and (b) schist, to illustrate the more regular cleavage direction in slate. Individual muscovite and biotite crystals are distinguished in the schist. Slate from Ballachulish, Argyll; schist from Lock Stack, Sutherland, Scotland.

## LAYERING, BANDING AND FABRIC DEVELOPMENT

23



Schematic block diagrams to illustrate the difference between S-tectonites (a) with a pronounced foliation (planar texture) and L-tectonites (b) with a pronounced lineation (linear texture). Metamorphic rocks such as schists and mylonites are generally L-S-tectonites, and have both a linear and planar component.

## PROCEDURE FOR MAKING THIN SECTIONS

### A. Materials needed

1. Hotplate with thermometer
2. Lakeside 70 *cement*
3. 27 mm x 46 mm glass slides
4. Glass plate
5. Grinding powders; 400, 600, 800, 1000 grit.

### B. Procedure

1. Using rock trim saw cut a rock chip about 1 inch square by 1/8 inch thick.
2. Score one side of a glass slide using 600 grit abrasive on a glass plate.
3. Heat hot plate to 140 degrees centigrade with slide and rock chip on the plate.
4. Apply a thin coat of Lakeside 70 to rock chip and place on scored side of glass slide. Remove from hot plate to cool.
5. Trim excess rock from the slide using the thin section saw.
6. Thin rock chip with thin section grinding wheel to approximate thickness.
7. Finish grinding thin section on glass plate with 800-1000 grit abrasives. Proper thickness will be reached when quartz appears gray to light straw yellow.

## RESULTS

*Your Results  
needs are  
noted due to my statement...*

1. Alaskite - ~~Phaneritic~~ igneous rock.  $\times$  Alaskite is distinguished from granite by its lack of darker minerals such as biotite.
2. Amygdaloidal basalt- ~~Porphyritic~~ igneous rock. This rock differs from normal basalt due to the amygdules which give it its porphyritic texture; the amygdules are formed by escaping mineral-rich water vapor that is released when the intrusion reaches the surface.
3. Augen gneiss. Higher levels of metamorphism causes schistosity to become less pronounced. Rock contains medium to coarse bands of differing texture and mineralogy (called gneissic banding) where light bands rich in quartz and feldspar alternate with darker ferromagnesian bands. Augen structures are also present in the rock, these are larger crystals of potassium feldspar arranged in a linear pattern parallel with the cleavage of the rock. Usually formed during regional dynamothermal metamorphism.
3. Metagabbro \ Gabbro is normally a phaneritic igneous rock; in this case it has been slightly metamorphosed to form porphyroblasts which are larger crystals surrounded by the groundmass of smaller equal sized grains. This was probably formed during a contact metamorphism where the temperature of the magma was maintained for a longer period of time.

4. **Mica schist - Coarse grained rock with excellent planar and linear schistosity.**  
Foliation present indicates a regional dynamothermal origin. Rock also contains porphroblasts of garnet.
5. **Mylonite - Fine-grained streaky rock with good schistosity. Mylonite resembles a very fine grained schist but it is actually formed during cataclastic metamorphism due to flowage of coarser rocks. Excellent indicator of seismic activity.**
6. **Phyllite - Fine-grained schistose rock formed at low temperature with high pressure during regional dynamothermal metamorphism.**



CITED REFERENCES

1. Barker, A. J., 1990, Introduction to ~~Metamorphic Texture and Microstructure~~; Blackie and son, New York, New York, pp. 21-103.
2. Conrad, S. G., 1958, Geologic ~~Map of North Carolina~~; North Carolina Department of Conservation and Development.
3. Fisher, Pettijohn, Reed, Weaver, 1970, Studies of Appalachian ~~Geology~~; John Wiley and Sons, pp. 195-271. *full names needed*
4. King, Philip, B., Ferguson, Lawrence, Roberts, 1944, Geology and ~~Manganese Deposits of Northeastern Tennessee~~; Division of Geology, State of Tennessee Department of Conservation.
5. Shelley, David, 1993, Igneous and ~~Metamorphic Rocks Under the Microscope~~; Chapman and Hall, New York, pp. 88-111.
6. Winkler, Helmut G. F., 1974, Petrogenesis of ~~Metamorphic Rocks~~; Springer Verlag, New York, New York, pp. 1-25.

*Numbered references not needed*

*You're not following model very well*

# **X-RAY ANALYSIS OF CAVE SEDIMENTS FROM PIGEON WATER CAVE OF NORTHEASTERN PINE MOUNTAIN**

---

**A Senior Thesis**

**Presented to**

**the Department of Physical Sciences**

**Morehead State University**

---

**In Partial Fulfillment**

**of the Requirements for**

**Science 471**

---

**by**

**Billy B. Stapleton**

**December 1992**

## X-RAY ANALYSIS OF CAVE SEDIMENTS FROM PIGEON WATER CAVE OF NORTHEASTERN PINE MOUNTAIN

STAPLETON, Billy B., Department of Physical Sciences,  
Morehead State University, Morehead, KY 40351

Pine Mountain extends 194 km in a northeast-southwest direction in eastern Kentucky and northeastern Tennessee and represents the northwestern edge of the Pine Mountain Overthrust Block. The Mountain's unique setting provides for unusual development of karst features in the Newman Limestone (the local equivalent of the Greenbrier-St. Genevieve-St. Louis limestones) which outcrops nearly half way up the mountainside on the west flank.

Pigeon Water Cave lies just 14.2 km south of Elkhorn City. Nearly 1 km in length, some passages reach 10 m in diameter and offer spectacular flowstone formations. Unlike other caves along Pine Mountain, Pigeon Water Cave has no visible surface stream entering its passages and contains very little siliciclastic debris. There exists, however, a subterranean stream in its lowest level which is believed by Belcher (1992, Personal Communication) to resurge as a spring nearly 70 m below its uppermost entrance.

The comparison of the X-ray analysis of fine-grained cave sediments with those of acid insolubles of the limestone along with direct observations made within the cave have shown that sediments exist primarily as autochthonous material (created within the cave from the solutioning of the limestone) with minor contributions from allochthonous sources (material transported into the cave).

## TABLE OF CONTENTS

	PAGE
INTRODUCTION .....	1
Purpose of Investigation .....	1
Geologic Setting .....	1
Stratigraphy .....	3
Cave Development .....	5
STUDY AREA .....	6
Location and Description of Cave .....	6
Sample Locations .....	9
LAB PROCEDURES .....	11
Initial Sample Preparation .....	11
Limestone Digestion .....	11
Initial Separation Procedures .....	12
Clay Extraction Procedures .....	13
Silt-Sand Separation Procedures .....	14
Clay Mounting Procedures .....	15
Treatment of Clays .....	16
X-RAY PROCEDURES .....	17
Equipment and Method .....	17
Identification of Minerals .....	17
Quantitative Analysis .....	19
RESULTS .....	21
Clay Analysis .....	21
Fraction Analysis .....	24
CONCLUSIONS .....	28
REFERENCES .....	30

## LIST OF FIGURES

FIGURE	PAGE
1. Map of Pine Mountain .....	2
2. Profile of Pine Mountain .....	3
3. Stratigraphic Column .....	4
4. Map of Pigeon Water Cave .....	7
5. Relation of Cave to Pine Mountain .....	8
6. Formulas Used for Quantitative Analysis ....	20
7. Peak Heights for Heat Treated Samples ....	21
8. Peak Heights for Glycolated Samples .....	21
9. Clay Composition of Cave Sediments .....	22
10. Clay Composition of Limestone Samples ....	22
11. Clay Composition Chart for All Samples ..	22
12. Plot of Average Clay Composition .....	23
13. Fraction Analysis of Limestone .....	24
14. Fraction Analysis of Cave Sediments .....	24
15. Lab Results from Fraction Analysis .....	25
16. Plot of Clay-Silt-Sand for All Samples ...	26

## INTRODUCTION

### Purpose of Investigation

This study is intended to provide a better understanding of cave sediments from limestone caves of northeastern Pine Mountain. A comparison of the X-ray analysis of fine-grained cave sediments with those of the acid insoluble fraction of the limestone will be made. This method of study has been shown to be useful in the determination of the origin of these fine-grained sediments (Frank, 1965). A general overview of the geologic setting and a look at the unique features of one of this mountain's many caves is given to acquaint the reader with the study area.

### Geologic Setting

Pine Mountain is a narrow crested, linear ridge that extends 194 kilometers in a northeast-southwest direction in southeastern Kentucky and northeastern Tennessee (Fig. 1). The mountain's spine-like crest represents the northwestern edge of the Pine Mountain Overthrust Block which is bounded on the southwest by the Jacksonboro Fault near Lafayette, Tennessee and on the northeast by the Russell Fork Fault near Elkhorn City, Kentucky. Peak elevations on this mountain range from 640 to 997 meters above sea level with reliefs of up to 488 meters, making it the most dominant

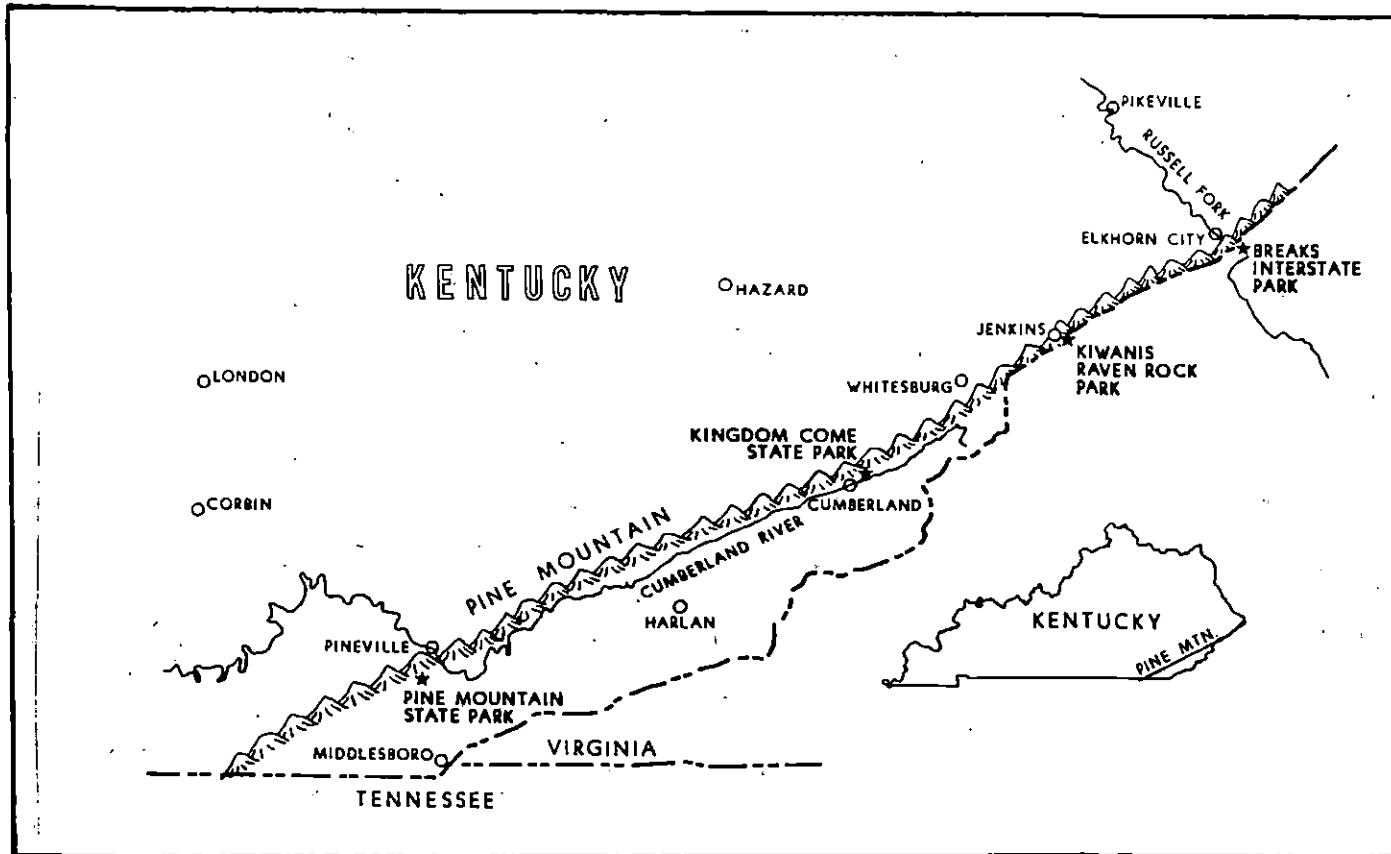


Figure 1. Map showing Pine Mountain and its location in relation to the rest of the state. (From Preston McGrain, 1975)

topographic feature in eastern Kentucky (Saunders, 1985, p. 87).

Streams cross the mountain in only two places: Clear Fork near Jellico, Tennessee, and the Cumberland River at Pineville, Kentucky. East of Pineville, the mountain stretches for 130 kilometers unbroken by any surface streams. Similarly, few roads give access across this natural barrier; only about a half dozen over its entire length.

### Stratigraphy

Pine Mountain's unique setting provides for unusual development of karst features in the Newman Limestone (the local equivalent of the Greenbrier-St. Genevieve-St. Louis Limestones) which outcrops nearly half way up the mountainside on the north flank (Fig. 2). This

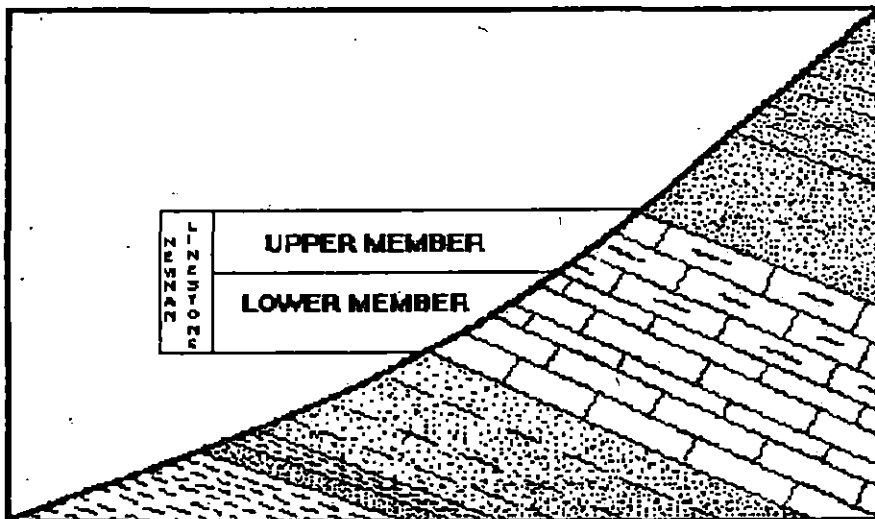


Figure 2. Profile of Newman Limestone as it outcrops on Pine Mountain. (NOT TO SCALE)



Mississippian limestone is composed of two units: the smaller upper member consisting of limestone, sandstone, and shale and a larger, lower limestone member (Fig. 3).

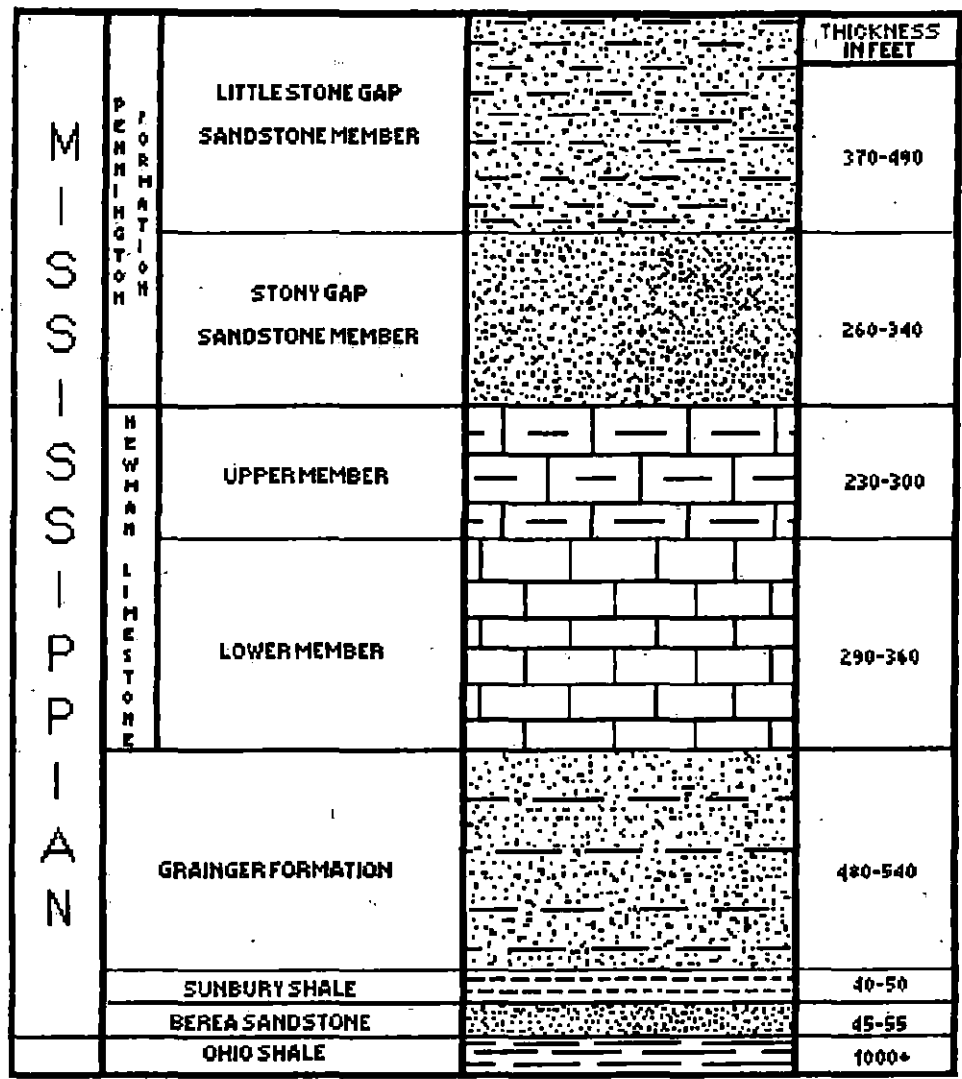


Figure 3. Stratigraphic profile of exposures on Pine Mountain. (NOT TO SCALE)

Along Pine Mountain the Newman Limestone is between 122 to 183m thick and dips into the mountain at 20 to 40 degrees (Saunders, 1985, p. 87).

Cave Development

Caves of Pine Mountain occur on the north face of the ridge and most if not all are located in the lower member. There are only nine mapped caves, but many more are known. They range in size from only a few meters to nearly 3km in length. Several pits are known as well, some in excess of 70m (Saunders, 1985, p. 89).

Many intermittent streams flow down the slope of the mountain, sinking into the limestone and resurging as springs at the lower contact of the limestone. Drainage in the limestone of the long mountains is from one direction only. Spring records are very sketchy, but drainage basins are up to 4,575m long and 460m wide (Saunders, 1985, p. 93).

## STUDY AREA

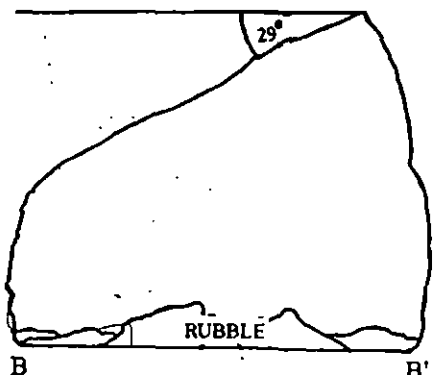
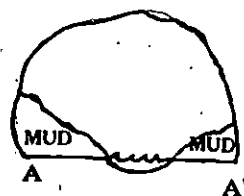
### Location and Description of Cave

Pigeon Water Cave lies 14.2km southwest of Elkhorn City, Kentucky and was chosen as the site for this investigation (Fig. 4). This cave compares to those described by Saunders (1985) in that it is relatively short in length and runs roughly parallel to the strike of the mountain (Fig. 5). Access to the cave is gained through either a hand dug upper entrance or a lower naturally formed entrance. The upper entrance is utilized most often due to its more direct access and the miserable crawl required by the lower access. The cave consists of a large main passage which reaches diameters in excess of 10m and a length of nearly .9km along with several smaller side passages barely large enough for a man to pass through. Both ends of the main passage are blocked by debris from ceiling failures, yet air can be felt emanating from beyond the blockage, indicating that the passage extends beyond.

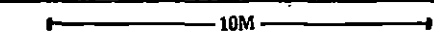
A lower partially water filled passage parallels the main passage. Only 60m of the underground stream is exposed due to sumps located on both the northeast and southwest ends. It is believed that this stream resurges as a spring near the lower entrance to the cave (Belcher, 1992, personal communication). A unique feature of this particular cave, in comparison to other caves of Pine Mountain, is the meager abundance of gravel in its stream channel. The stream in

CROSS SECTION A-A'

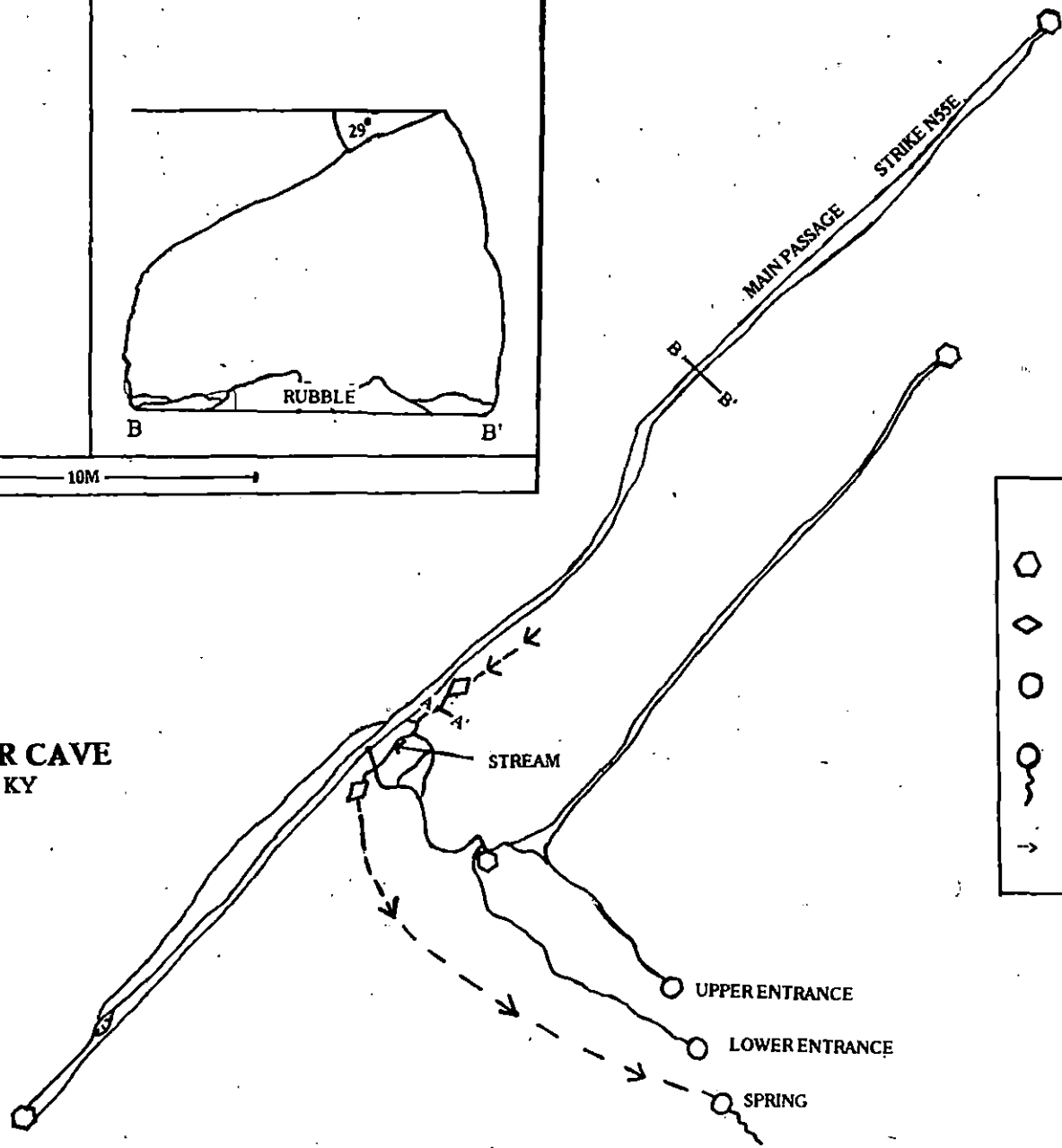
CROSS SECTION B-B'



SCALE



**PIGEON WATER CAVE**  
LOWER PIGEON, KY



**LEGEND**

- BREAKDOWN (BLOCKAGE)
- SUMP
- ENTRANCE
- SPRING
- FLOW DIRECTION

SCALE  
(IN METERS)

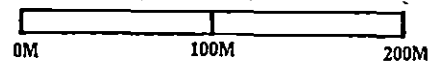


Figure 4. Map of Pigeon Water Cave (By: Bill Stapleton).

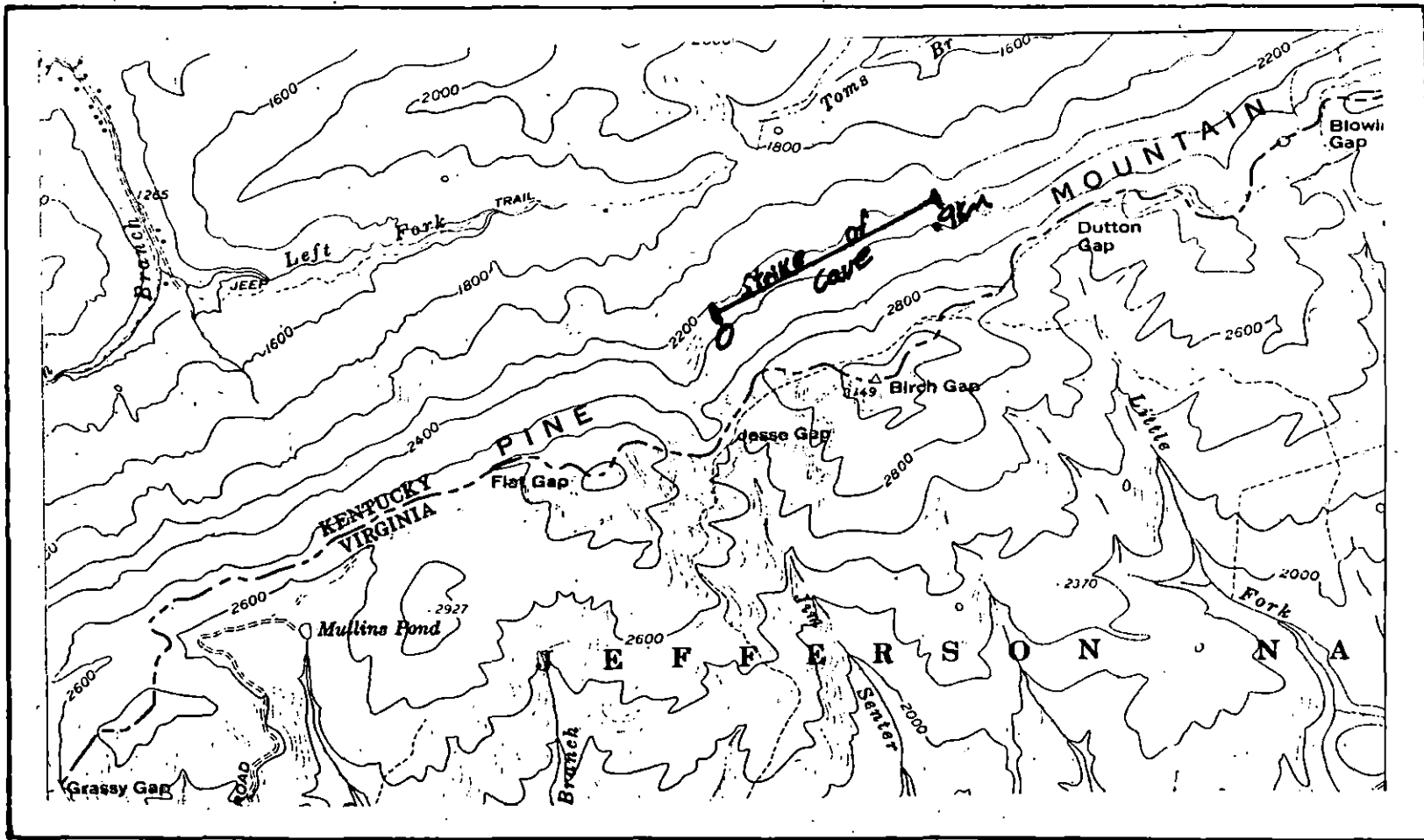


Figure 5. Map showing relation of Pigeon Water Cave to Pine Mountain. (From USGS 7.5 Minute Clintwood Quadrangle)

Pigeon Water Cave carries very little gravel, but an enormous amount of mud as evidenced by its chest-high mud banks (Fig 5, A-A', pg. 7).

The solutioning of the main passage appears to have been bedding controlled due to the uniformly sloping ceiling which strikes N52°E and dips 29°SE, correlating to the dip of the strata along Pine Mountain. The lower stream passage follows a fracture striking the same direction which permits access to the upper main passage.

Throughout the cave, large and impressive speleothems add to the majesty of this undeveloped cave. Travertine dams, stalagmites, stalagmites, and flowstone structures are found in great abundance and are for the most part undamaged by human hands.

Sample Locations

Limestone samples were gathered from four separate sites. The first site (Q1) was from the active quarry at Elkhorn Stone Company 3.8km southwest of Elkhorn City. The second sample (Q2) was taken from an abandoned quarry at Ashcamp, 8.9km southwest of Elkhorn City. The third and fourth samples (Q3a and Q3b respectively) were taken from the limestone outcrop at the upper entrance of Pigeon Water Cave. Approximately 5kg of fresh sample was collected at each site after removing the weathered surface, thus allowing access to unweathered rock.

Cave sediment samples were collected from the lower stream passage of the cave. Four sampling points located approximately 15m apart were established on both the east and west sides of the stream for a total of eight samples. Approximately 1kg of mud was collected from the mud banks at each site after removing the weathered surface. These samples were labeled E1-E4 for the east side and W1-W4 for the west (E1 and W1 being the extreme upstream sampling points). All samples were then carefully sealed and transported to the geology lab at Morehead State University.

## LAB PROCEDURES

### Initial Sample Preparation

Once in the lab, all sediment samples were removed from their individual sample bags and placed in appropriately labeled porcelain dishes. Each of the four limestone samples were first crushed using a mechanical rock crusher and placed in similarly labeled porcelain dishes. All samples were then placed in a 75°C oven and allowed to dry thoroughly.

### Limestone Digestion

Limestone digestion was carried out using a modified version of Peterson's method (1962, p.13) developed by Robert Lierman (1992, personal communication). A representative sample of each limestone was ground using a mortar and pestle and then sifted through a No. 20 sieve overlaying a No. 140 sieve. The particles caught by the No. 140 sieve were used for the digestion process. This was done so as to increase the surface area and hasten digestion. An acid solution was prepared in a 500ml Erlenmeyer flask for each of the 4 samples by mixing 8ml of concentrated acetic acid with 50ml of Calcium Acetate. Distilled water was then added to make a 450ml .3M solution. Acetic acid was used instead of hydrochloric to prevent damaging any chlorite minerals which may be present in the samples. Calcium Acetate simply acts as a buffer to



maintain a pH of 4.5-5.5 which prevents the acid from attacking clay minerals. 20g of each sample was then placed in its appropriately labelled flask and allowed to dissolve overnight. The following day, the liquid was decanted off and fresh solution added to reconstitute the 450ml solution. This process was repeated three times to insure an adequate amount of clays for processing, yet the digestion was not allowed to go to completion in order to prevent any possible damage to the clays by the acid. After the third run, the acid solution was decanted off and the sample washed thoroughly with distilled water.

#### Initial Separation Procedures

In order to determine the relative composition of the sample in terms of grain size distribution, it was first necessary to separate the grains within each sample. This was accomplished by placing the entire sample of the partially dissolved limestone in a *Proctor-Silex* commercial blender along with 100ml of tap water. The sample was then blended at high speed for approximately 2 minutes. The process was repeated for each of the samples. The sediment samples underwent the same process differing only in that 10g of the dry sediment was added to the blender.

All samples then underwent a process to remove any iron which can unfavorably affect the results from X-ray analysis. After each sample was blended, the slurry was placed in a properly labelled centrifuge jar and centrifuged

for 10 minutes at 2500rpm. If the water was cloudy after centrifuging,  $\text{CaCl}_2$  was added to flocculate the clays and the sample was again centrifuged. The water was then gently poured off and 70ml of .3M Na-Citrate and 5ml of Na-Bicarbonate was added to the jar and placed in a low temperature oven. After 15 minutes, 1/8 teaspoon of Sodium Hydroxide was added and the sample heated for 15 minutes longer. This process leaches out the iron from the sample and places it in suspension (Lierman, 1992, personal communication). The sample was then allowed to cool and was centrifuged for 10 minutes at 2500rpm. The liquid was then poured off and the sample was ready for separation.

#### Clay Extraction Procedures

Clay extraction was carried out in the same centrifuge jars by applying Stokes Law calculated for a withdraw depth of 8.5cm for particles  $<.004\text{mm}$ . Because settling time is temperature dependent, a table of values calculated by Lierman (1992, personal communication) for the desired withdraw depth was used.

Each jar was filled with distilled water, capped, and shaken vigorously until well mixed. The jars were then placed under a sonic dismembrator for 1 minute to deflocculate clays. The jars were placed on a stable platform and allowed to settle according to the time as calculated from the table.

After sufficient time had elapsed, the liquid was drawn off using a vacuum apparatus to a depth of 8.5cm and placed in an appropriately labelled plastic beaker. This constitutes the clay sized fraction of the sample. The process was repeated three times or until the upper 8.5cm of liquid in the centrifuge jar was clear. Approximately 2.5ml of  $\text{CaCl}_2$  was added to the beaker in order to flocculate the clays. The beaker containing the clays was then centrifuged for 10 minutes at 2500rpm in order to concentrate the clays. The liquid was decanted and the clays allowed to dry.

#### Silt-Sand Separation Procedures

The sediment remaining in the centrifuge jars after clay extraction represents the silt and sand size ( $>.004\text{mm}$ ) fraction of the sample. Because the limestone samples were not allowed to completely digest, the larger than clay size fraction of the sample was placed in a 10% HCl solution and allowed to dissolve completely so that an accurate insoluble content could be determined. After complete digestion, the clays were extracted using the same method as above, but were kept separate from the first run and were not used for clay analysis. However, its weight was added to the first run in determining the total acid insoluble content of the limestone.

The  $>.004\text{mm}$  fraction of each sample was first washed through a No. 230 mesh sieve. The particles caught by the sieve represent the sand size ( $>.0625\text{mm}$ ) fraction of the

sample. The sieve was labelled and placed in a low temperature oven where it was allowed to dry completely.

The particles passing through the sieve remain in suspension and represent the silt size (between .004mm and .0625mm) fraction of the sample. The suspension was then filtered through standard filter paper so as to catch all particles. The filter paper containing the silts was then allowed to dry.

Each fraction (clay, sand, and silt) was then weighed and weights recorded for each sample as well as percent composition.

#### Clay-Mounting Procedures

Clays were prepared for X-ray analysis by mounting as elutriated samples on glazed glass slides. Two identical mounts per sample were prepared for a total of 24 elutriated samples. Two additional pack samples were prepared by powdering the dried clays with a mortar and pestle and packing them into a sample holder. The two pack samples were chosen at random, one from the limestone suite and the other from the sediment suite.

The elutriated samples were prepared by first cutting biological microscope slides in half and lightly glazing one side so the clays would more easily adhere to the surface. A .3g sample of the dried clays was weighed out, placed in a vial along with 4ml of distilled water, and allowed to hydrate for several minutes. The sample was then mixed

thoroughly by a laboratory vibrator, placed under the sonic dismembrator for 2 minutes, removed and mixed again by the vibrator. The sample was then split into 2 equal volumes. The clay suspensions were mounted by dripping them onto the glazed surface of their respective slide by using glass syringes. The freshly prepared slides were allowed to dry beneath an infrared lamp before they were moved.

#### Treatment of Clays

One slide of the sample pair was heat treated to 180°C for one hour prior to X-ray analysis. The remaining slide was treated with ethylene glycol. Considerable difficulty was encountered in the glycolation process. Initially the samples were treated by applying a uniform coat of the ethylene glycol with a dropper. This tended to cause the clays to loose cohesion to the glass and peel up. A second attempt was made to glycolate the samples by placing them in an enclosed evaporation apparatus so that the samples would become saturated from the ethylene glycol vapors. Because this method requires that the samples be heated slightly in the presence of the vapors, the clays again lost cohesion with the glass. Finally, the clays were successfully glycolated by spraying the ethylene glycol from a fine mist spray bottle onto the sample. Two light coats were applied, allowing the sample to air dry in-between coats.

## X-RAY PROCEDURES

### Equipment and Method

All samples were X-rayed using a Phillips Model No. XRG-2500 X-ray Diffractometer utilizing CuK radiation in conjunction with a Phillips chart recorder. A baseline of 1.0, multiplier of 5, scan speed of  $1^\circ 2\theta/\text{min.}$ , and a chart speed of  $1^\circ/\text{min.}$  was used for all runs.

The first step in X-ray analysis is to identify the minerals one can expect to encounter throughout the investigation. This was accomplished by first running the 2 untreated pack samples from  $4^\circ 2\theta$  through  $60^\circ 2\theta$ , thus allowing the major peaks of most clay minerals to be expressed.

### Identification of Minerals

Peaks from X-ray charts were identified through the use of transparent overlays marked with the reflection angles from most major clay minerals in both degrees  $2\theta$  and  $\text{\AA}$  units. In some instances, the Powder Diffraction File published by the Joint Committee for Powder Diffraction Standards (1974) was consulted.

After identification of the major peaks from the pack samples, it was determined that illite, kaolinite, chlorite, and quartz were common to all samples. Montmorillinite was suspected, but because it commonly occurs as a mixed layer,

assemblage with illite, its existence could not be confirmed until after running the ethylene glycol treated samples (Grim, 1968, p. 438). Elutriated samples were then ran from  $2^{\circ}2\theta$  through  $30^{\circ}2\theta$  in order to detect major reflections of the common minerals.

In referring to montmorillinite, the term is used to describe all expandable clays with the exception of vermiculite (Grim, 1968, p. 41). Montmorillinite expands readily to about  $18\text{\AA}$  when solvated with ethylene glycol. Kaolinite was defined as clay minerals which show both  $3.58\text{\AA}$  and  $7\text{\AA}$  peaks. Illite refers to the clay mineral with a  $10\text{\AA}$  basal spacing which is not significantly expanded after solvating with ethylene glycol (Robbins and Keller, 1952, p. 148). Chlorite is represented by a basal reflection at  $3.58\text{\AA}$  (Griffin, 1971, p. 555). Quartz peaks lie at  $3.34\text{\AA}$  and  $4.26\text{\AA}$ .

The purpose of treating the samples with ethylene glycol, as previously mentioned, is to determine the existence of expandable clays. Glycolation tends to cause the crystalline lattice of expandable clays to expand, thus changing the reflection pattern of the X-rays. Heat treatment of the samples to  $180^{\circ}\text{C}$  for 1 hour tends to collapse the clays, thus sharpening their corresponding peaks (Grim, 1968).

X-ray analysis took place over a <sup>two</sup> 2-day period. After all peaks were identified and labeled, a baseline was drawn so that peak heights could be measured relative to baseline.

## Quantitative Analysis

The study performed by R.M. Frank in 1965, in which he concluded that the clay content of cave sediments could be used to differentiate their source, requires a method of quantifying the clays in the sample. George M. Griffin along with his former colleagues from Shell Development Laboratories developed a simplified method of quantitative analysis (Fig. 6). By measuring characteristic peak heights in a sample, the percent composition of clays could be obtained.

Before applying this method, three assumptions must first be made (Griffin, 1971, p. 554):

1. The reported clay minerals (kaolinite, chlorite, illite, and montmorillinite) comprise 100% of the sample, whereas in many cases there are other minerals present as well as amorphous material.
2. The refracting ability of the clay minerals is constant.
3. There is a 1:1 linear relationship between the ratio of the 3.58Å kaolinite peak to the 3.54Å chlorite peak.

Peak heights must be measured in millimeters from baseline for the 7Å, 10Å, 3.54Å, and 3.59Å peaks of the heat treated samples. The 7Å and 10Å peak heights from the glycolated samples are required as well. After these peak heights are obtained for each sample, it is simply a matter of plugging the values into the appropriate equations to determine clay percentages. In this case, calculations were performed by a personal computer running *Microsoft Work's Spreadsheet for Windows*.



The following assumptions must be made:

1. The reported clay minerals comprise 100% of the sample.
2. The refracting ability of the clay minerals is consistent.
3. There is a 1:1 linear relationship between the ratio of the 3.58 Å kaolinite peak to the 3.54 Å chlorite peak.

(a) On the 180°C pattern, measure the heights of the 7 and 10 Å peaks. Calculate the total percent kaolinite and/or chlorite as follows:

$$\% K + C = \frac{\frac{h_{7\text{Å}}(180^\circ)}{2.5}}{\frac{h_{7\text{Å}}(180^\circ)}{2.5} + h_{10\text{Å}}(180^\circ)} \times 100$$

(b) On the 180°C pattern measure the heights of the 3.54 and 3.59 Å peaks. These heights are used to apportion the 7 Å peak into percent kaolinite and percent chlorite as follows:

$$\% K = \frac{h_{3.59\text{Å}}(180^\circ)}{h_{3.59\text{Å}}(180^\circ) + h_{3.54\text{Å}}(180^\circ)} \times \% K + C$$

$$\% C = (\% K + C) - \% K$$

(c) Calculate the total percent illite and/or montmorillonite as follows, using peak heights from the 180°C pattern:

$$\% I + M = \frac{h_{10\text{Å}}(180^\circ)}{\frac{h_{7\text{Å}}(180^\circ)}{2.5} + h_{10\text{Å}}(180^\circ)} \times 100$$

(d) Measure the 7 and 10 Å peak heights on the ethylene glycol pattern. Use these measurements and the previous ones on the 180°C pattern to calculate percentages of illite and montmorillonite as follows:

$$\% I = \frac{h_{10\text{Å}}(\text{EG}) \left( \frac{h_{7\text{Å}}(180^\circ)}{h_{7\text{Å}}(\text{EG})} \right)}{h_{10\text{Å}}(180^\circ)} \times \% I + M$$

$$\% M = (\% I + M) - \% I$$

Figure 6. Formulas used for quantitative clay analysis.  
(From George M. Griffin)

## RESULTS

### Clay Analysis

Figures 7 and 8 show measured peak heights of heat treated samples and glycolated samples, respectively. These values were used in calculating relative clay composition using the formulas from figure 6 (See p. 20). The results from these calculations are shown separately for cave sediments and limestone insolubles in figures 9 and 10, respectively. Figure 11 shows all results graphically.

PEAK HEIGHTS FOR 180 C SAMPLES (MILLIMETERS FROM BASELINE)													
	<u>E1</u>	<u>E2</u>	<u>E3</u>	<u>E4</u>	<u>W1</u>	<u>W2</u>	<u>W3</u>	<u>W4</u>	<u>Q1</u>	<u>Q2</u>	<u>Q3A</u>	<u>Q3B</u>	<u>AVERAGE</u>
3.54A	99	123	110	89	113	114	110	116	82	97	70	52	97.9
3.59A	119	149	123	105	150	139	119	115	76	97	76	51	109.9
7A	75	81	85	88	89	86	72	71	51	61	54	43	71.3
10A	155	189	183	122	211	212	192	185	117	151	156	110	165.3

Figure 7. Measured peak heights for heat treated samples.

PEAK HEIGHTS FOR GLYCOLATED SAMPLES (MILLIMETERS FROM BASELINE)													
	<u>E1</u>	<u>E2</u>	<u>E3</u>	<u>E4</u>	<u>W1</u>	<u>W2</u>	<u>W3</u>	<u>W4</u>	<u>Q1</u>	<u>Q2</u>	<u>Q3A</u>	<u>Q3B</u>	<u>AVERAGE</u>
7A	42	52	47	58	52	30	38	45	38	45	32	30	42.4
10A	53	70	62	70	73	30	36	57	64	87	70	56	60.7

Figure 8. Measured peak heights for glycolated samples.

<b>CLAYS NORMALIZED TO 100% (CAVE SEDIMENTS)</b>									
	<u>E1</u>	<u>E2</u>	<u>E3</u>	<u>E4</u>	<u>W1</u>	<u>W2</u>	<u>W3</u>	<u>W4</u>	<u>AVERAGE</u>
% KAOLINITE	8.8	8	8.3	12.1	8.2	7.7	6.8	6.6	8.3
% CHLORITE	7.4	6.6	7.4	10.3	6.2	6.3	6.2	6.7	7.1
% ILLITE	51.2	49.3	51.7	67.6	50.7	34.9	30.9	42.1	47.3
% MONT.	32.6	36.1	32.6	10	34.9	51.1	56.1	44.6	37.3

Figure 9. Clay composition analysis for cave sediments.

<b>CLAYS NORMALIZED TO 100% (L.S. ACID INSOLUBLES)</b>					
	<u>Q1</u>	<u>Q2</u>	<u>Q3A</u>	<u>Q3B</u>	<u>AVERAGE</u>
% KAOLINITE	7.1	6.9	6.4	6.7	6.8
% CHLORITE	7.7	7	5.8	6.8	6.8
% ILLITE	62.5	67.2	66.5	63.1	64.8
% MONT.	22.7	18.9	21.3	23.4	21.6

Figure 10. Clay composition analysis for limestone samples.

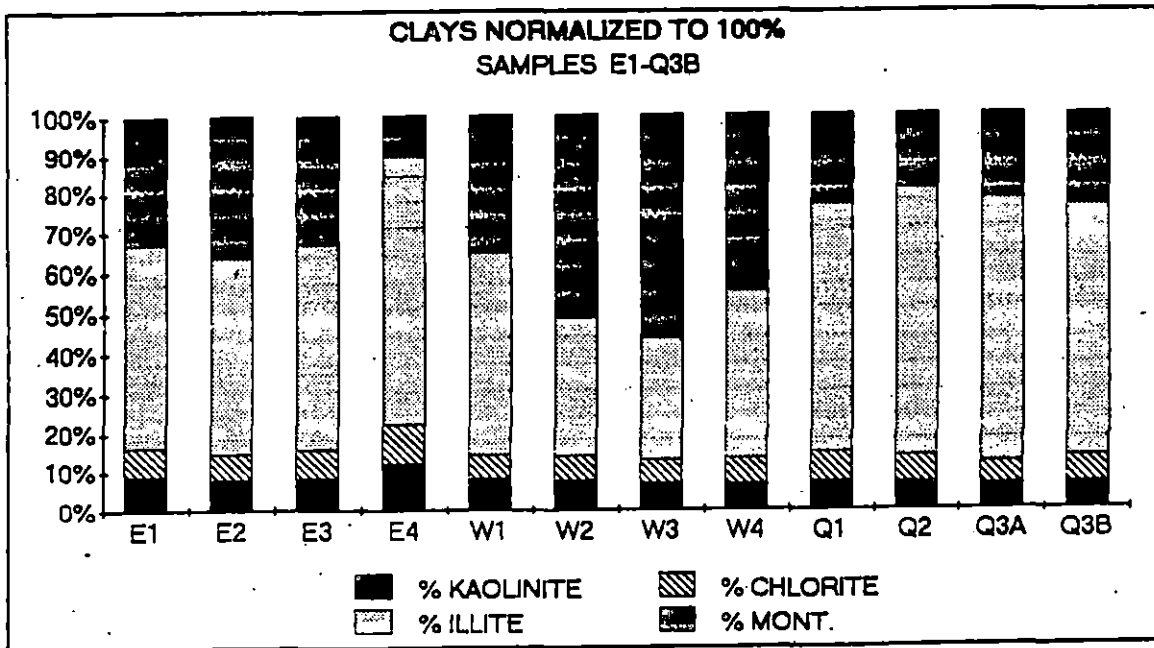


Figure 11. Graph showing clay composition for all samples.

To simplify the results, the average composition of the cave sediment suite is compared to the average composition of the limestone suite. The cave sediments were found to contain 8.3% kaolinite, 7.1% chlorite, 47.3% illite, and 37.3% expandable montmorillinite. In comparison to the cave sediments, the limestone samples contained 6.8% kaolinite, 6.8% chlorite, 64.8% illite, and 21.6% montmorillinite. By plotting the percentages, a definite correlation between the two suites becomes evident (Fig. 12).

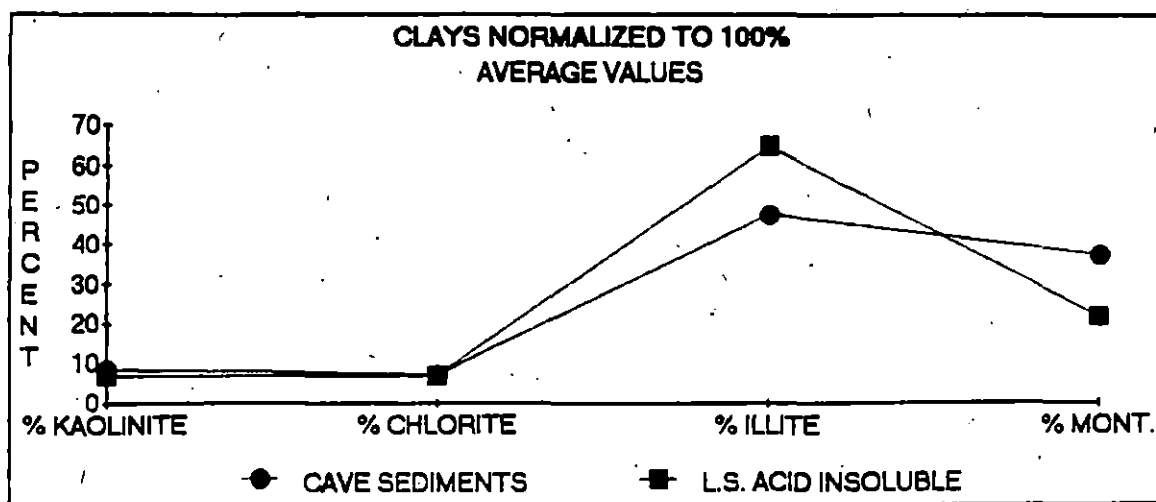


Figure 12. Plot of average values for clays.

Though there appears to be some slight variation between the two suites in illite and montmorillinite composition, it can most likely be explained by the fact

that illite can become altered through physical and chemical processes involved with the solutioning of limestone (Ford and Williams, 1989, p.329). Naturally, the cave sediments have endured a great deal more weathering than the limestone, thus altered clays such as montmorillinite would be more abundant in the sediments.

#### Fraction Analysis

Digestion of the limestone proved it to be on the average of 68.8% pure carbonate, leaving 31.2% insoluble residue. Of the insoluble material from the limestone, 10% was clay, 68.1% was silt, and 21.9% was sand (Fig. 13). In contrast, cave sediments yielded 25.7% clay, 50% silt, and 24.3% sand (Fig. 14). Actual lab results for each sample are given in Figure 15.

<b>FRACTION ANALYSIS OF SAMPLES Q1-Q3B (NEWMAN LIMESTONE)</b>					
	<u>Q1</u>	<u>Q2</u>	<u>Q3A</u>	<u>Q3B</u>	<u>AVERAGE</u>
<u>%CLAY</u>	8.9	14.8	8.1	8.4	10
<u>% SILT</u>	75.7	80.9	62.1	53.6	68.1
<u>% SAND</u>	15.4	4.3	29.8	38	21.9

Figure 13. Fraction analysis from limestone samples.

<b>FRACTION ANALYSIS OF SAMPLES E1-W4 (PIGEON WATER CAVE)</b>									
	<u>E1</u>	<u>E2</u>	<u>E3</u>	<u>E4</u>	<u>W1</u>	<u>W2</u>	<u>W3</u>	<u>W4</u>	<u>AVERAGE</u>
<u>%CLAY</u>	27.2	25.3	25.3	21.7	24.4	24.5	28.9	28.5	25.7
<u>% SILT</u>	44.1	55.2	51.4	50.3	43.9	52.5	54.3	48.4	50
<u>% SAND</u>	28.7	19.5	23.3	28	31.7	23	16.8	23.1	24.3

Figure 14. Fraction analysis from sediment samples.

FRACTION ANALYSIS FOR SAMPLES E1-Q3B					FRACTION ANALYSIS FOR SAMPLES E1-Q3B						
SAMPLE	DESCRIPTION	SAMPLE WEIGHT	ACID INSOLUBLES	% INSOLS	SAMPLE	CLAY	%CLAY	SILT	% SILT	SAND	% SAND
E1	Sediment	10g	N/A	N/A	E1	2.72 g	27.2	4.41 g	44.1	2.87 g	28.7
E2	Sediment	10g	N/A	N/A	E2	2.53 g	25.3	5.52 g	55.2	1.95 g	19.5
E3	Sediment	10g	N/A	N/A	E3	2.53 g	25.3	5.14 g	51.4	2.33 g	23.3
E4	Sediment	10g	N/A	N/A	E4	2.17 g	21.7	5.03 g	50.3	2.80 g	28.0
W1	Sediment	10g	N/A	N/A	W1	2.44 g	24.4	4.39 g	43.9	3.17 g	31.7
W2	Sediment	10g	N/A	N/A	W2	2.45 g	24.5	5.25 g	52.5	2.30 g	23.0
W3	Sediment	10g	N/A	N/A	W3	2.89 g	28.9	5.43 g	54.3	1.68 g	16.8
W4	Sediment	10g	N/A	N/A	W4	2.85 g	28.5	4.84 g	48.4	2.31 g	23.1
Q1	Newman Limestone	20g	5.85 g	29.3	Q1	.52 g	8.9	4.43 g	75.7	.9 g	15.4
Q2	Newman Limestone	20g	5.75 g	28.8	Q2	.85 g	14.8	4.65 g	80.9	.25 g	4.3
Q3a	Newman Limestone	20g	7.05 g	35.3	Q3a	.57 g	8.1	4.38 g	62.1	2.1 g	29.8
Q3b	Newman Limestone	20g	7.11 g	35.5	Q3b	.6 g	8.4	3.81 g	53.6	2.7 g	38

Figure 15. Lab results from fraction analysis.

A plot of the clay, silt, and sand fractions for both suites depicts a nearly consistent distribution within the cave sediments (Fig. 15). However, there is variation within the limestone suite. Samples Q1 and Q2 show higher percentages of silt with a lesser amount of sand in both samples. An attempt to explain why there is a difference within the suite would require more intensive study of the limestone. However, one explanation could lie in the fact that the two samples (Q1 and Q2) were collected as far as 10km from the study area, lending the possibility of a lithologic change within the limestone over this distance.

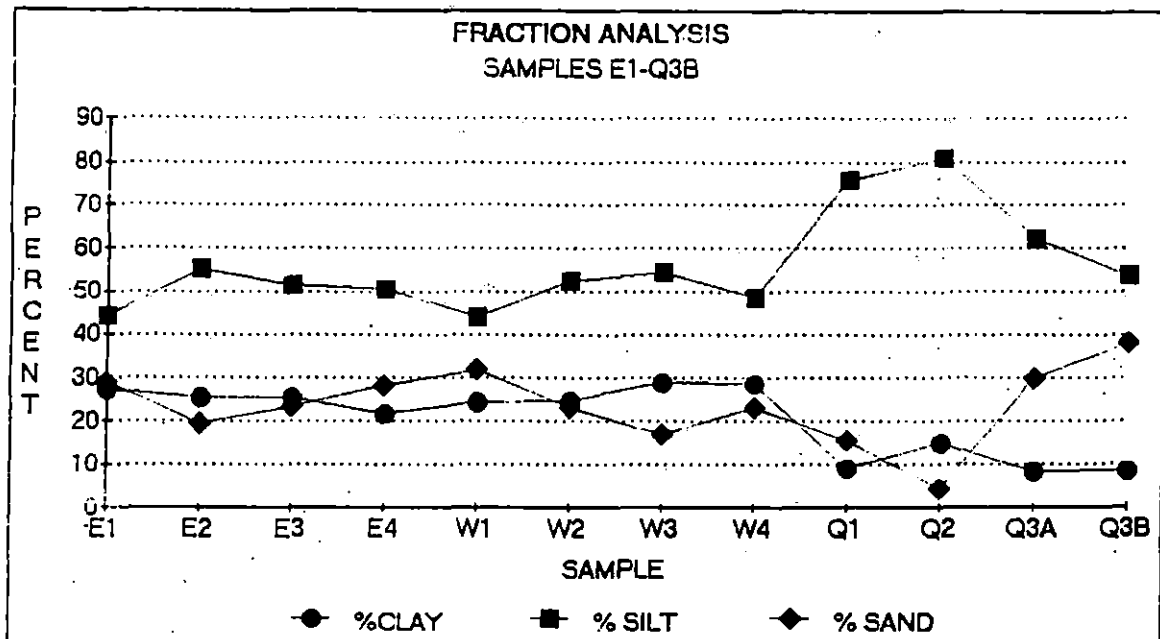


Figure 16. Plot of clay-silt-sand for all samples.

Considering only the samples taken at the study area (Q3a and Q3b), there is still variation between the two suites. There tends to be a higher percentage of silt in the limestone samples, and lesser amounts of clays in comparison to the sediment samples. It could be argued that the variance between the suites is due to the fact that the sediments have undergone more weathering than the analyzed limestone, thus resulting in the breakdown of the larger fractions into clay size material. This seems a likely proposal.



## CONCLUSIONS

Drawing from the results of the fraction analysis, it depicts a definite correlation between the insoluble fraction of the limestone and that of the cave sediments in terms of grain size distribution. The small variance can be accounted for by the differences in weathering experienced between the limestone and the sediment samples. This gives evidence to the theory that these sediments are autochthonous in nature.

Perhaps the strongest evidence for the sediments being derived from the solutioning of the limestone lies in the results of the X-ray analysis. As in Franks's study (1965), a definite relationship exists between the clay minerals of the limestone and those of the cave sediments. Though there is slight variation between samples, again the variation can be pinned on differences in weathering.

In making the determination of the origin of these fine-grained sediments, one more line of evidence must be considered. The stream bed in Pigeon Water Cave does possess a limited amount of quartz gravel. Because the Newman Limestone is overlain by the Pennington Formation, which consists of sandstone and conglomerate units, one can hazard that the gravel is being carried into the cave from the overlying unit. If gravel is being carried into the cave, then other sediment is as well. However, because the overlying members were not considered in this study, an

explanation for the distribution of these sediments will not be offered.

In conclusion, the sediments encountered in the stream passage of Pigeon Water Cave are a mixture of both allochthonous and autochthonous sediments. Gravel in the streambed indicates that sediment is being transported into the cave system. But, because of the strong evidence provided by X-ray and fraction analysis, an overwhelming percentage of the fine-grained sediments must be considered autochthonous.

Because no visible surface stream enters the cave system, a dye trace of the mountain southwest of Pigeon Water Cave would be of great benefit to similar future studies. Also, analysis of overlying units would be highly recommended.

## SELECTED REFERENCES

- Belcher, K.R. (1992) Personal communication.
- Commonwealth of Virginia (1963) Clintwood Quadrangle, 7.5 Minute Series: U.S. Geological Survey Topographic Quadrangle.
- Ford, D.C. and Williams, P.W. (1989) Karst Geomorphology and Hydrology: Unwin Hyman, London.
- Frank, R.M. (1965) Petrologic study of sediments from selected central Texas caves: MA Thesis, University of Texas, Austin.
- Griffin, G.M. (1971) Interpretation of x-ray diffraction data: in Carver, R.E., ed., Procedures in Sedimentary Petrology: John Wiley and Sons, New York.
- Grim, R.E. (1968) Clay Mineralogy: McGraw-Hill, New York.
- Joint Committee on Powder Diffraction Standards (1974) Selected Powder Diffraction Data for Minerals: JCPDS, Philadelphia.
- Lierman, Robert. (1992) Personal Communication: Former Assistant Professor of Geology, Morehead State University.
- McGrain, Preston (1975) Scenic Geology of Pine Mountain in Kentucky: Kentucky Geological Survey, University of Kentucky, Lexington.
- Peterson, M.N.A. (1962) The mineralogy and petrology of upper Mississippian carbonate rocks of the Cumberland Plateau of Tennessee: Jour. Geology, vol.70, p. 1-31.
- Robbins, C. and Keller, W.D. (1952) Clay and other noncarbonate minerals in some limestones: Jour. Sed. Petrol., vol.22, p. 146-152.
- Saunders, J.W. (1985) Pine Mountain karst and caves: in Caves and karst of Kentucky: Kentucky Geol. Survey, Special Publication 12, Series XI, p.86-96.

**THE CORRELATION OF STREAM-  
DEPOSITED BRECCIAS  
IN BAT CAVE,  
CARTER CAVES, KENTUCKY**

---

**A Senior Thesis Presented to the  
Department of Physical Sciences  
Morehead State University**

---

**In Partial Fulfillment of the  
Requirements for the  
Degree of Bachelor of Science  
in Geology**

---

by

**James Bond**

**October, 1993**

## TABLE OF CONTENTS

ABSTRACT.....	iii.
INTRODUCTION.....	1
LOCATION OF STUDY.....	2.
General Stratigraphy.....	2.
CAVE FORMATION.....	7.
Cave Interior Deposits.....	8.
General Sedimentation.....	8.
Speleothem Growth.....	9.
Travertine Deposits.....	9.
Cave Breccias.....	9.
METHODS OF INVESTIGATION.....	11.
Brunton Compass and Hand Level.....	11.
Presence of Travertine Deposits.....	11.
Comparison to Modern Analogs.....	12.
RESULTS.....	13.
Breccia One.....	13.
Breccia Two.....	13.
Breccia Three.....	14.
DISCUSSION.....	17.
REFERENCES CITED.....	19.

*parcels  
not  
necessary*

## TABLE OF FIGURES

Figure 1. Map of Bat Cave.....	3.
Figure 2. Outline Map Showing Geological Regions and Location of the Carter and Cascade Region.....	4.
Figure 3. Geologic Time Scale Showing the Age of the Rocks in Carter <i>County</i> with those in the rest of Kentucky.....	5.
Figure 4. Sketch Showing the Relationship of the Outstanding Features of Carter Caves State Park with the Geologic Formations.....	6.
Figure 5. Map of Bat Cave Showing Location of Breccias.....	15.
Figure 6. Relative Positions of Stream Deposited Breccias in Bat Cave.....	16.

## THE CORRELATION OF STREAM DEPOSITED BRECCIAS IN BAT CAVE, CARTER CAVES, KENTUCKY.

BOND, James A., Department of Physical Sciences, Morehead State University, Morehead, KY 40351

Bat Cave, located at Carter Caves State Resort Park in Olive Hill, KY, was the location of this study. Bat Cave is a limestone cave formed by dissolution of limestone by water. In this study, an attempt was made to correlate stream deposited breccias that occur throughout the cave. Breccias were correlated using a Brunton Compass and a hand level. Speleothem growths, travertine deposits, and relative vertical position were used to determine relative ages of cave deposits.

Three distinct breccias were found, indicating three distinct stream levels. Breccia One is at the current stream level where deposition is still active. Breccia Two is located approximately three to six feet above present stream level. Breccia Two displayed speleothem growth locally, which suggests this breccia has been inactive for some time. Breccia Three is the oldest breccia and is located in the upper passage of the cave. Breccia Three is covered by a thicker travertine deposit than locally coats Breccia Two. Locally, ancient travertine dam deposits occur at the same level as Breccia Three.

Ancient breccias were compared to modern breccia found at present stream level. Both modern and ancient breccias showed fining upward sequences. Upward fining indicates that stream channels were abandoned.

Ancient breccias can be used to constrain paleo-climate. For example, in order for a breccia to form, the stream must remain at one level in the cave for a fairly long period of time. This means that if water flow is too great, the stream does not deposit its load, and rapid down cutting will occur. The rapid down cutting lessens the time for deposition. On the other hand, if there is not enough water there will be no stream and no deposition. The formation of the fining upward breccia indicates flow waned. The decreased flow was due to channel abandonment (e.g. form stream down cutting to deeper level) or, more likely, due to a glacial cycle when the water is tied up in the ice.

### PRIMARY REFERENCES

Ford, Derek, Williams, Paul, 1989, Karst Geomorphology and Hydrology, Academic Division of Unwin Hyman Ltd., 15/17 Broadwick Street, London, pp. 242-355.

McGrain, Preston, 1966, Geology of the Carter and Cascade Cave Areas, Kentucky Geological Survey, University of Kentucky, Special Publication 12, pp. 6-13.

Tierney, John, 1985, Caves of Northeastern Kentucky (With Special Emphasis on Carter Caves State Park), in Caves and Karst of Kentucky, edited by Percy H. Dougherty, Kentucky Geological Survey, Special Publication 12, Series XI, pp. 78-84.

White, William B., 1988, Geomorphology and Hydrology of Karst Terrains, Oxford University Press, New York, New York, pp. 220-300.

## INTRODUCTION

*Triples  
Space  
Area*

The study of cave sedimentation can give clues to ancient long-term climatic changes. Speleothem growth can be dated radiometrically providing accurate dates that can indicate periods of growth and non-growth in the formation (Moore and Sullivan, 1964).

Fluvial deposits can give clues to water levels and velocities. All these factors can contribute to an overall better understanding of paleoclimate.

This study was conducted in an attempt to correlate and relative-age date the various levels of stream deposited breccia in Bat Cave. Once the number of distinct levels of breccia and their relative ages is determined, it becomes possible to make inferences about stream velocity and the amount of time the stream remained at one level in the cave.



## LOCATION OF STUDY

*Triple Upper  
Water Reservoir*

This study was conducted in Bat Cave, located at Carter Caves State Resort Park in Olive Hill, KY.

*Leaves  
sent: well  
passage  
not part*

Bat Cave, as shown in Figure 1, is one of the largest caves on the park with approximately 3.35 km of passageways (Tierney, 1985). The cave is made up of two levels that run roughly parallel to one another. The lower level of the cave constitutes the main passageway, having wide rooms and high ceilings. A stream, Cave Branch, runs through this level making it susceptible to periodic flooding. The upper level is somewhat smaller and usually drier. Flood water only rarely reaches the upper level. There is, however, some speleothem growth in this level that is lacking in the lower level.

*Triple Upper  
Space ( ... out before )*

## General Stratigraphy

Carter Caves is located in the northern portion of the Eastern Coal Field of Kentucky (see Figure 2). The hills and ridges are capped by a massive sandstone from the Pennsylvanian Period, called the Lee Sandstone (McGrain, 1966). Underlying the sandstone are layers of limestone dating back to the Mississippian Period. They include the Lower Chester, Ste. Genevieve, and St. Louis limestones (see Figure 3). It is in these limestones the caves of Carter Caves <sup>have</sup> form. Bat Cave itself is formed primarily in the Ste. Genevieve and St. Louis Limestones (McGrain, 1966).

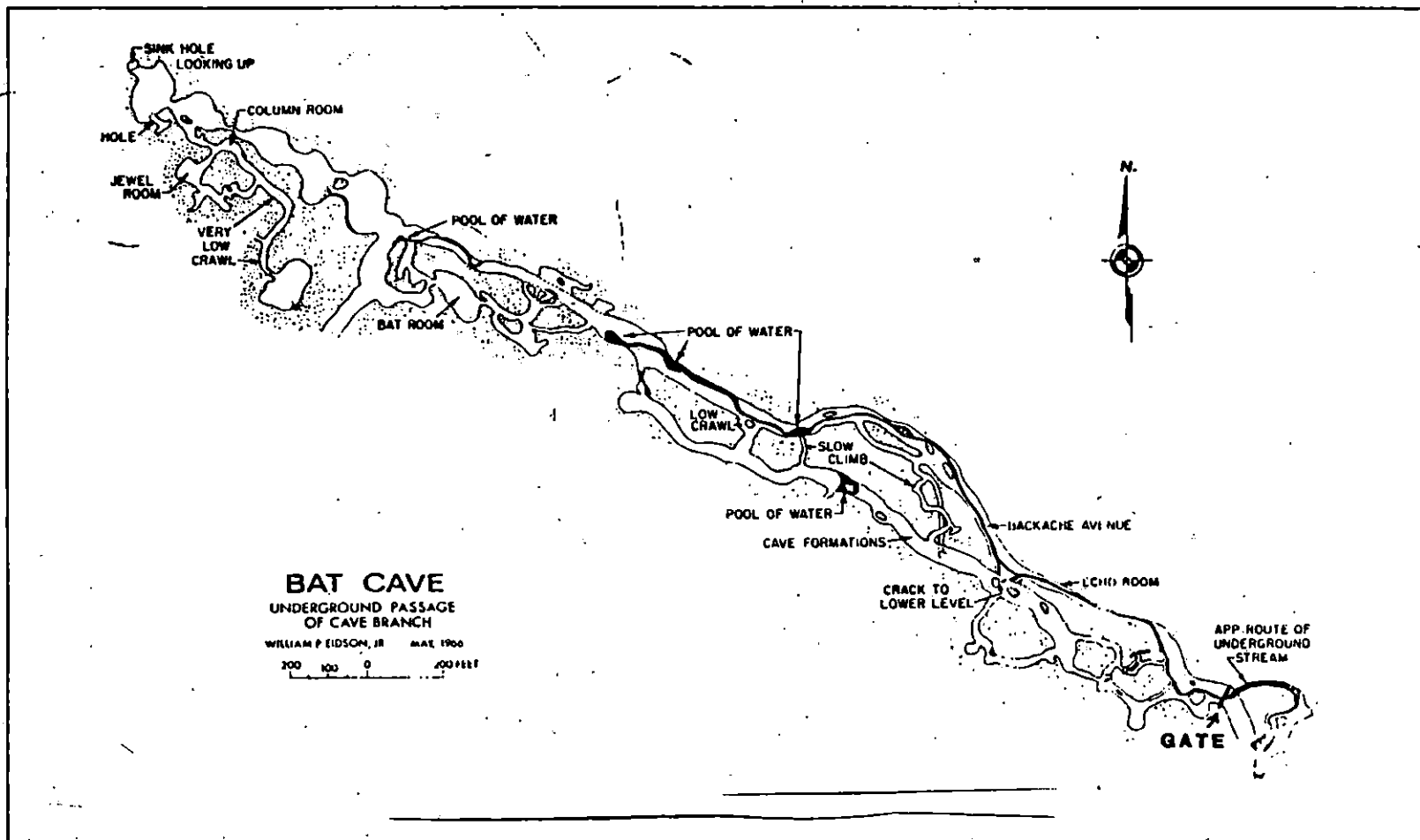


Figure 1. Map of Bat Cave (From Tierney, 1985).

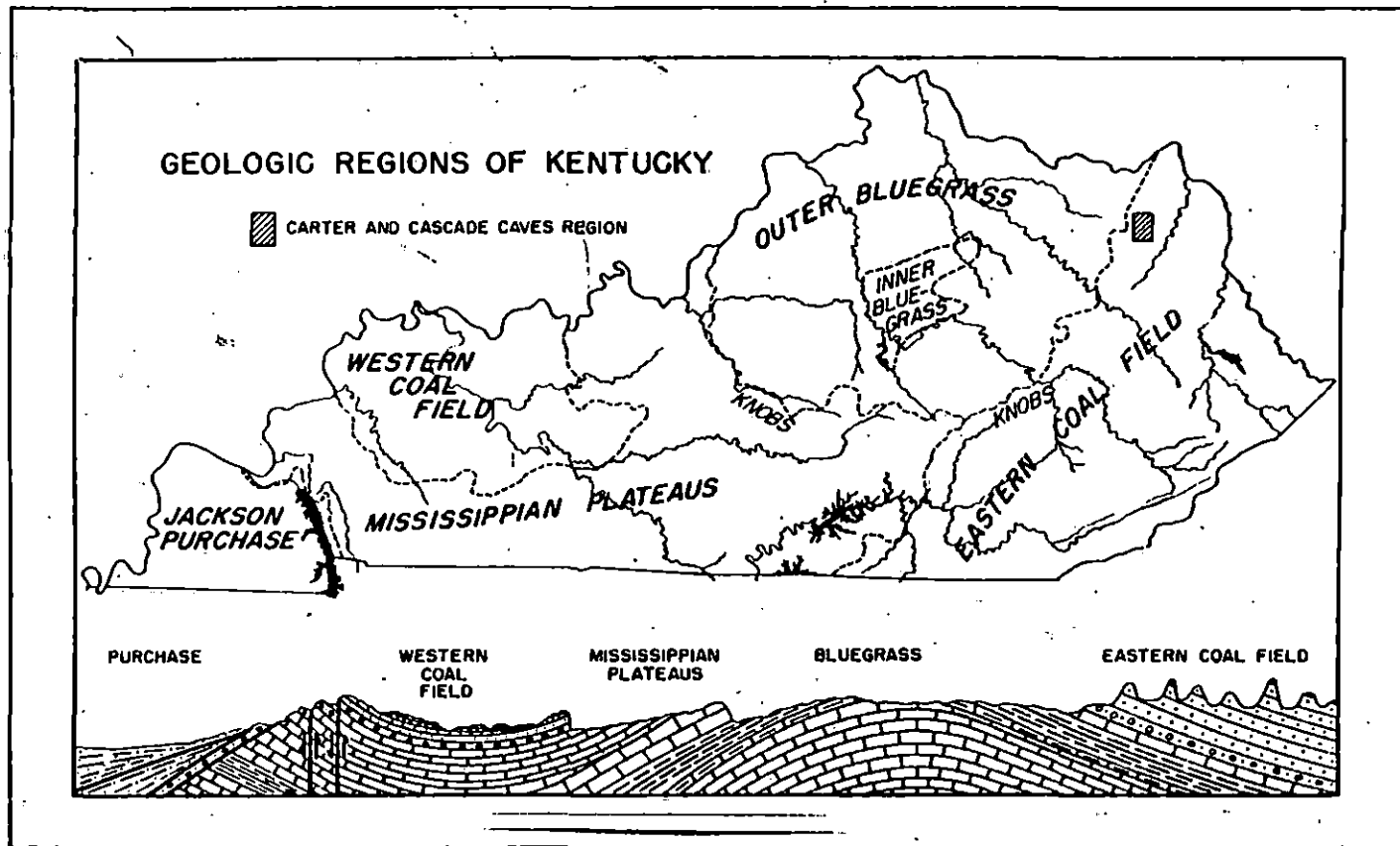


Figure 2. Outline map of Kentucky showing geologic regions and location of the Carter and Cascade region (From McGrain, 1966).

ERA (DURATION IN MILLIONS OF YEARS)	ROCKS EXPOSED IN		PERIOD (DURATION IN MILLIONS OF YEARS)	AGE (MILLIONS OF YEARS)
	KENTUCKY	CARTER CO.		
GENOZOIC 64±	[Hatched pattern]	[Blank]	QUATERNARY	1
			TERTIARY	62
MESOZOIC 167±	[Blank]	[Blank]	CRETACEOUS	72
			JURASSIC	46
			TRIASSIC	49
			PERMIAN	50
PALEOZOIC 370±	[Hatched pattern]	[Vertical lines]	PENNSYLVANIAN	30
			MISSISSIPPIAN	35
	[Blank]	[Blank]	DEVONIAN	60
			SILURIAN	20
			ORDOVICIAN	75
			CAMBRIAN	100
PRE-CAMBRIAN 4,000±	[Wavy pattern]	[Blank]		4,600

Figure 3. Geologic calendar showing the relation of the ages of the rocks in Carter County with those in the rest of Kentucky (From McGrain, 1966).

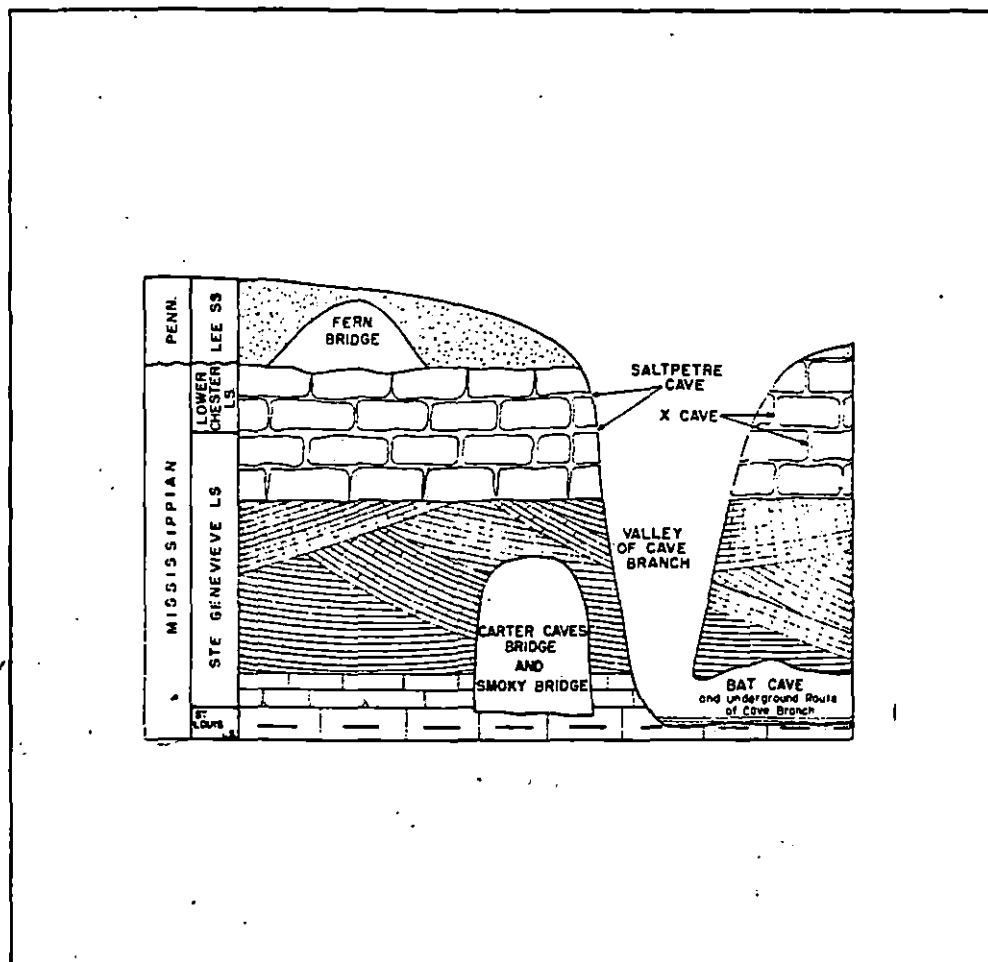


Figure 4. Sketch showing the relationship of outstanding features of Carter Caves State Park with the geologic formations (FromMcGrain, 1966).

## CAVE FORMATION

The most widely accepted definition of a cave is: any natural hole in the rock large enough for a person to enter and achieve total darkness (Ford and Williams, 1989).

Caves can be formed by several mechanisms. They can be formed by dissolution, erosion, volcanic activity, glacial activity, tectonic activity, or some combination of these factors. In northeastern Kentucky, caves are generally formed through the dissolution of carbonate rocks. The dissolution reactions usually involve carbonic acid, although other acids, such as sulfuric acid from oxidation of pyrite or dissolution of hydrogen sulfide gas in water, have been shown to be important in some cases (White, 1988).

Large scale structural elements such as folds and faults also help control cave development. In areas with strongly folded rocks, the caves tend to form parallel to axial planar cleavage or axial joint sets. Caves that form in steeply dipping beds, along major fractures, or along major faults, tend to have a strong vertical component (White, 1988). In other words, they form as tall, narrow corridors.

In Carter County the carbonate bedrock is nearly horizontal and soluble horizons extend horizontally in two dimensions. Therefore, tributaries tend to aggregate but remain within the same stratigraphic horizon. This permits complex drainage systems to develop (White, 1988).

## **Cave Interior Deposits**

*Trampel  
Space*

### **General Sedimentation**

*Trampel  
Space*

Caves function as giant sediment traps, accumulating a variety of clastic, organic, and chemical debris. They are often the most varied deposits that form in continental environments and they tend to be preserved for greater spans of time than most other deposits (Ford and Williams, 1989).

Cave sediments are generally classified into two main categories; clastic sediments and chemical sediments. Clastic sediments include, among other things, fluvial deposits, organic debris, and breakdown, which is debris from roof collapse. Chemical sediments include travertines, speleothems, and ice (White, 1988).

Clastic sediments can be very complex. The law of superposition states that in areas of flat lying rock, the oldest rock unit was laid down first and is therefore on the bottom of the stratigraphic section (Prothero, 1990). This law is often violated due to slumping, burrowing, and flowstone intrusion. Rates of deposition can even vary due to cave collapse blocking off down stream areas for long periods of time and then finally being eroded away to allow deposition to occur once more. If the cave is prone to frequent and severe flooding there can be a great deal of reworking and redeposition of sediments (Ford and Williams, 1988).

### ***Speleothem Growth***

The word "speleothem" is a term used to describe cave formations due mainly to the precipitation of calcite. Speleothems include formations such as stalactites, stalagmites, flowstones, soda straws, and rimstone dams (Ford and Williams, 1988).

Speleothem consist mainly of calcite deposited from dripping water. As water from the surface percolates through the limestone above the cave, it dissolves calcite. When it reaches the interior of the cave the water deposits its calcite (Moore and Sullivan, 1964). The deposition is triggered by a loss of CO<sub>2</sub> from the water.

Caves that experience frequent flooding tend to lack speleothem growth because the flood waters wash away any calcite precipitant that may have formed. Bat Cave has very little speleothem growth in the lower level where flooding is common.

### ***Travertine Deposits***

Travertine is calcium carbonate that is deposited under atmospheric conditions (Klein and Hurlbut, 1993). Travertine deposits are found as different formations. It can be deposited as travertine dams, which impound water. It can also be deposited as a coating on ceilings, walls, and formations.

### ***Cave Breccias***

Cave breccias form just like normal stream breccias. As the stream carries its load, some of the gravel, sand, silt, and clay becomes deposited with the larger gravels being eventually cemented together by the smaller particles. A typical sequence of breccia will



fine upward (James and Choquette, 1988 ). This is due to the fact that as water flow is reduced due to processes such as meandering, cut off, and abandonment, the larger particles will settle out first, followed by the sands, silts, and finally clays.

## METHODS OF INVESTIGATION

In this study, an attempt was made to identify and correlate the various levels of stream breccia in Bat Cave. Three methods were used: 1.) Brunton compass and hand level, 2.) the presence of travertine deposits, 3.) comparisons to modern analogs.

### Brunton Compass and Hand Level

With the Brunton compass and hand level, an attempt was made to determine if any two breccia deposits, both within sight of one another, were in fact the same layer. This was done by shooting a sight level with one breccia to the other. This method allowed breccia deposits to be traced laterally through the cave over large distances.

### Presence of Travertine Deposits

The presence of travertine deposits covering a breccia deposit suggested the breccia was older than any breccias lacking travertine deposits. It could, however, suggest that the area where the breccia with the travertine was found was simply more conducive to speleothem growth.

### Comparison to Modern Analogs

Comparison to modern analogs was done to help determine if the paleo-breccias were stream deposits or solution collapse breccias. Stream deposits should show some sorting and a fining upward sequence. Solution collapse breccia, on the other hand, would not show any sorting.

The current stream level breccia was dug into revealing a cross-section. The breccia did, in fact, show fairly good sorting and a fining upward sequence. This information was then compared to the paleo-breccias.

## **RESULTS**

There were three distinct levels of breccia found in Bat Cave (see Figures 5 and 6). Two were found in the lower level of the cave and the third was found in the upper level.

### **Breccia One**

Breccia One was the current stream level breccia. It was found throughout the lower level of the cave, from entrance to exit. The thickness ranged from 0 meters to approximately 1 meter. It contained sandstone and chert clasts and displayed a fining upward sequence. The last centimeter contains thin clay laminations. There were no travertine deposits found anywhere on this breccia. This breccia was the youngest of the three due to its position in the cave and the lack of any travertine deposits.

### **Breccia Two**

Breccia Two was also found in the lower level of the cave. It was found throughout much of the main passageway and in several side passages. In general it ran parallel to and above the current stream direction. The height of breccia two above floor level varied from .5 meters to 2.5 meters. Breccia Two displayed a fining upward sequence with sandstone

and chert clasts. The upper contact was topped by clay laminations. Breccia Two displays thin coatings of travertine in some locations.

### **Breccia Three**

Breccia Three was found in the upper level of the cave near the ceiling. It was a layer 10 to 15 cm thick and it was only traceable for about 2.5 meters. The clasts were well sorted and coated with much thicker travertine deposit than Breccia Two. Directly across from Breccia Three were a group of clay laminations that appeared to be rimstone dam deposits as part of the dam was still evident. Breccia Three was the oldest of the three breccias found. This was due to its position in the cave and the presence of thick travertine deposits.

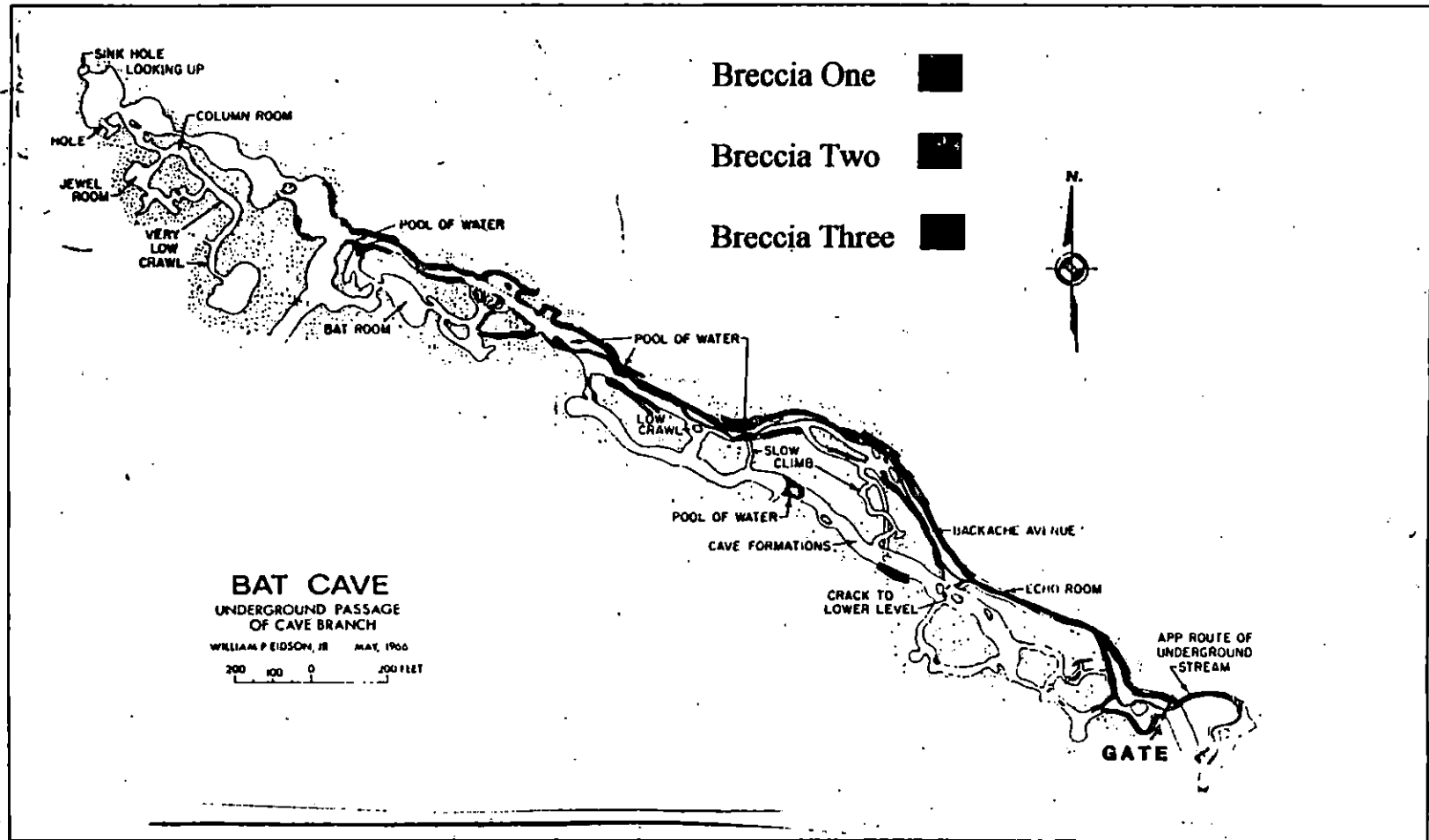


Figure 5. Map of Bat Cave showing location of breccias (After Tierney, 1985).

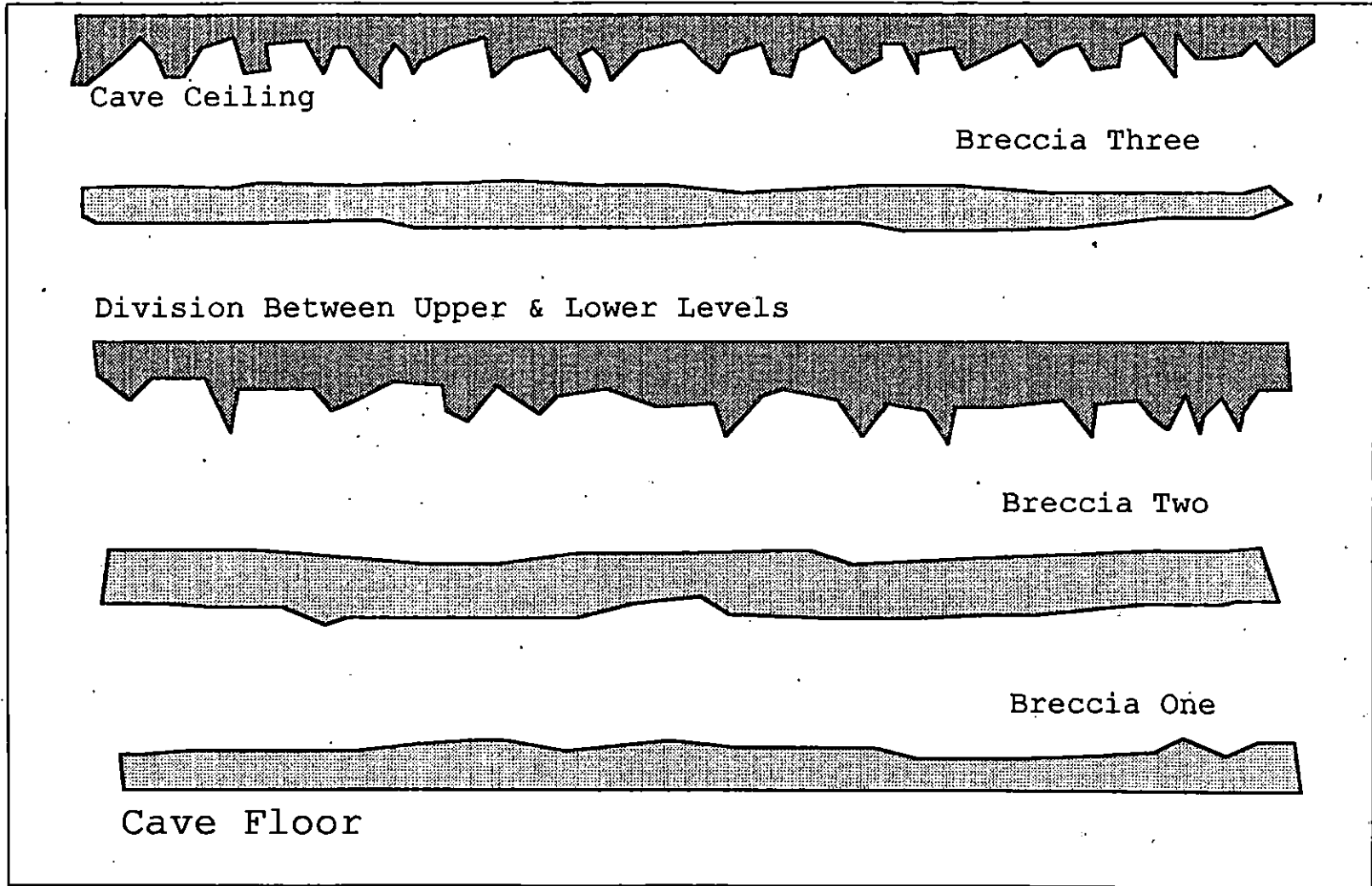


Figure 6. Relative positions of stream deposited breccias in Bat Cave, Carter Caves State Park (not to scale).

## DISCUSSION

The cave was formed due to the chemical and mechanical effects of Cave Branch. The three levels of breccia indicated three times when the stream remained at one level in the cave for an extended period of time, since it takes some time for the breccia to form. This was most likely due to a reduction of the flow velocity of the stream. Such a reduction would lessen the down cutting effect of the stream and force the stream to remain in place.

These reductions in flow velocity were then followed by a sudden increase in flow velocity causing the stream to inundate the cave and down cut rapidly. This influx of water prevented the stream from forming breccia deposits.

The most likely cause of these fluctuations in stream velocity is glaciation. During periods of glacial transgression more water is tied up in the ice. This had the affect of reducing the stream velocity in the cave to the point of eliminating it. As the glaciers melted it would produced a great influx of glacial outwash. This outwash served to greatly increase stream velocities and increase the down cutting effect of the water. It was, I believe, during interglacial periods that the breccias were deposited. During these times stream flow was not be too weak to carry sediment or to strong to rapidly down cut. It was, therefore, possible to deposit the breccias found in Bat Cave.

The most accurate way to attempt to tie the cave breccias to glaciation would be through radiometric dating of the speleothems found in the cave. The speleothems should show increased growth during periods of glacial retreat and decreased growth during glacial advance. The radiometric dating would provide actual dates to be compared with known



dates of glaciation. This could then be compared to the cave breccias to determine if they do, in fact, correlate. Radiometric dating was not done in this study due to time and money constraints, however, it would make an interesting project in the future.

## REFERENCES CITED

- Ford, Derek, <sup>and</sup> Williams, Paul, 1989, Karst Geomorphology and Hydrology, Academic Division of Unwin Hyman Ltd, 15/17 Broadwick Street, London, pp. 242-355.
- James, N.P., <sup>and</sup> Choquette, P.W., 1988, Paleokarst, Springer-Verlag, New York, New York, pp. 1-10.
- Klein, Cornelis, <sup>and</sup> Hurlbut, Cornelius S., 1993, Manual of Mineralogy, John Wiley & Sons, New York, New York, pp. 579.
- McGrain, Preston, 1966, Geology of the Carter and Cascade Cave Areas, Kentucky Geological Survey, University of Kentucky, Special Publication 12, pp. 6-13.
- Moore, George W., <sup>and</sup> Sullivan, G. Nicholas, 1964, Speleology: The Study of Caves, Cave Books, St. Louis, MO, pp. 41-63.
- Prothero, Donald R., 1990, Interpreting the Stratigraphic Record, W.H. Freeman & Company, New York, New York, pp. 331.
- Tierney, John, 1985, Caves of Northeastern Kentucky (With Special Emphasis on Carter Caves State Park), in Caves and Karst of Kentucky, edited by Percy H. Dougherty, Kentucky Geological Survey, Special Publication 12, Series XI, pp. 78-84.
- White, William B., 1988, Geomorphology and Hydrology of Karst Terrains, Oxford University Press, New York, New York, pp. 220-300.

JOINTING AND FAULTING IN  
SELECTED AREAS OF  
EASTERN KENTUCKY

---

A Research Paper  
Presented to the  
Department of Physical Sciences  
Morehead State University

---

In Partial Fulfillment  
of the Requirements for  
Science 471

---

by  
Mark A. Blair  
December 13, 1993

## TABLE OF CONTENTS

	PAGE
INTRODUCTION.....	1
General Definition of Terms.....	2
METHODS OF INVESTIGATION AND CORRELATION.....	6
Methods of Investigation.....	6
Methods of Correlation.....	11
POSSIBLE CAUSES OF JOINTING AND FAULTING.....	16
Possible Causes of Jointing.....	16
Possible Causes of Faulting.....	18
ECONOMIC SIGNIFICANCE OF THIS STUDY.....	20
CONCLUSIONS.....	21
WORKS CITED.....	22

## LIST OF FIGURES

FIGURE	PAGE
1. Locations of Study.....	1
2. Diagram of Joint.....	3
3. Systematic and Non-Systematic Joints.....	3
4. Strike-Slip Fault.....	4
5. Dip-Slip Fault.....	4
6. Oblique-Slip Fault.....	4
7. Fault Subcategories.....	5
8. Video Enhancer Set-up.....	7
9. Television Monitor.....	7
10. Projection of Satellite Imagery.....	9
11. Lineament Tracing on Map.....	9
12. Rose Diagram.....	13
13. Rose Diagram Showing Two Joint Sets.....	13
14. Irvine-Paint Creek Fault.....	14
15. Satellite Imagery/Direct Measurement Rose Diagram Comparison.....	15
16. Sequence Leading up to Jointing and Faulting.	19



*cutts*

## General Definition of Terms

The definitions of jointing and faulting are relatively simple. A joint is defined as a fracture in strata in which no displacement has taken place (Figure 2). There are two classifications of jointing. These are termed as systematic and non-systematic. These joints form a joint system. The angle between the joints is about 90 degrees. The difference between the two is that systematic joints are more continuous and linear than non-systematic joints (Figure 3).

Faulting can merely be defined as a joint in which displacement has taken place. Faults can be classified by slip sense. Slip sense is defined as the direction of slip. The three ways faults are classified are strike-slip, dip-slip, and oblique-slip faults. Strike-slip faults are faults that have slipped in a horizontal direction (Figure 4). This is exemplified by the famous San Andreas Fault in California. The second type of fault is the dip-slip fault. Dip-slip faulting occurs in a vertical plane (Figure 5). All of the faults in this study were of this type. The last category of faulting is oblique-slip faulting. Oblique-slip

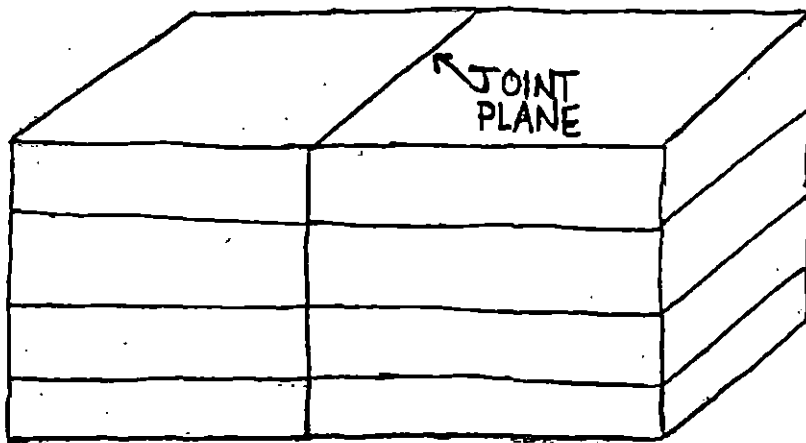


Figure 2: Block Diagram of joint, showing joint plane.

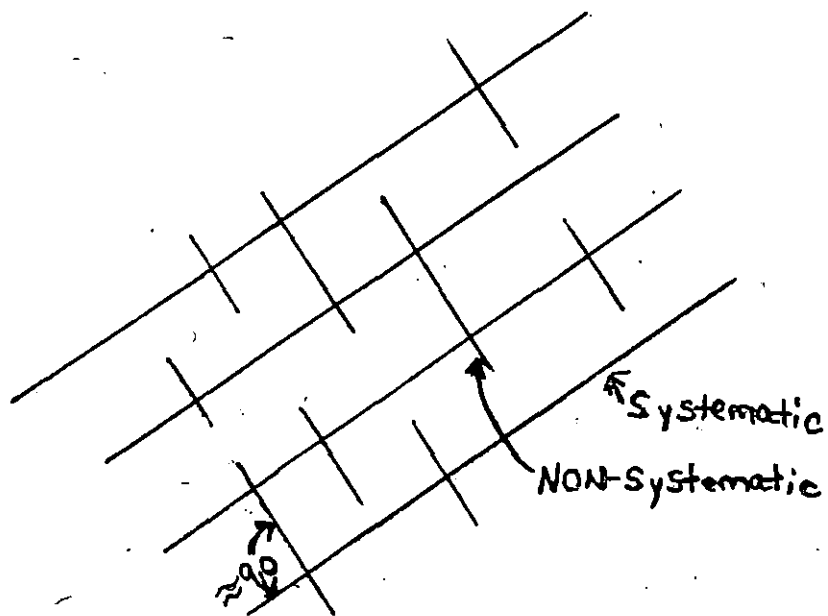


Figure 3: Systematic and Non-systematic joint system.



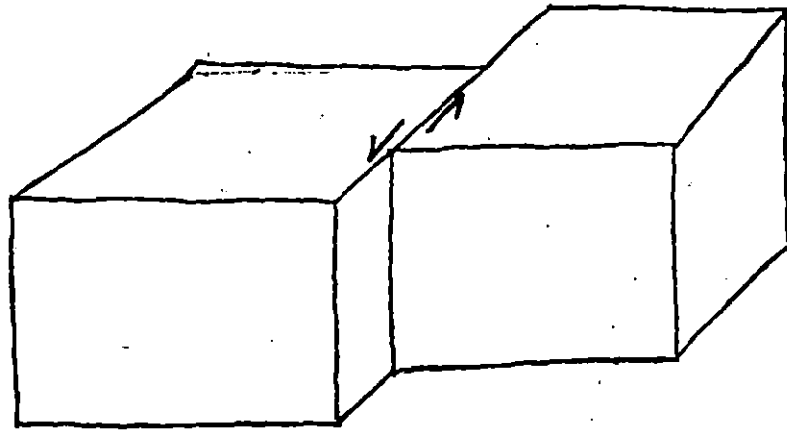


Figure 4: Strike-Slip Fault, arrows show relative movement.

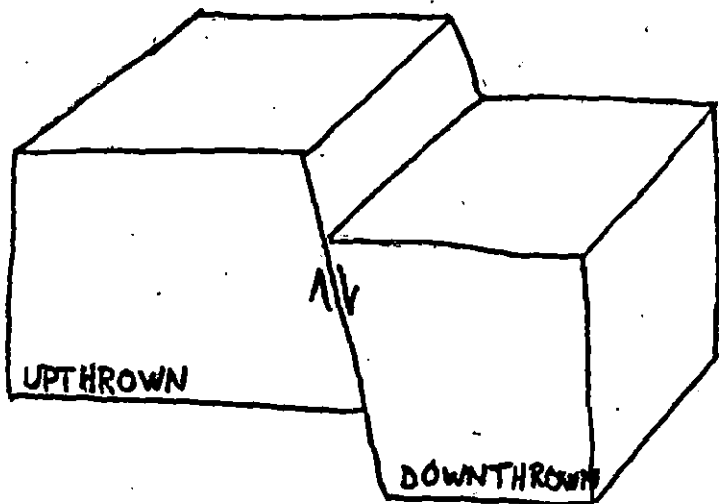


Figure 5: Dip-Slip Fault, arrows show relative movement.

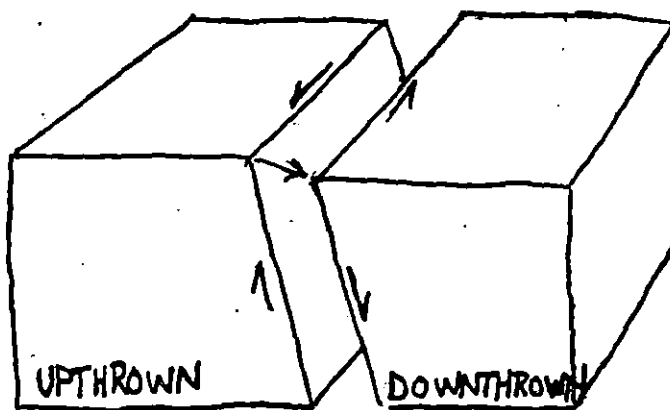


Figure 6: Oblique-Slip Fault, arrows show relative movement.

faults show movement in both the horizontal and vertical directions(Figure 6).

Faulting can be further divided into subcategories as shown in figure seven. For the purposes of this research the only subcategories of concern are normal and reverse faulting. Only dip-slip and oblique-slip faults can be divided in this manner. A normal fault is formed due to strain while a reverse fault is caused by pressure. A reverse fault can also be termed as a thrust fault. This is important due to the fact that knowing the direction in which forces were acting gives clues to the causes. This topic will be addressed later in more detail (Dennis, 1987, p197).

### FAULT CLASSIFICATION BY SLIP SENSE

#### STRIKE-SLIP FAULTS

Right-slip fault  
Left-slip fault

#### DIP-SLIP FAULTS

Normal-slip fault  
Reverse-slip fault

#### OBLIQUE-SLIP FAULTS

Right-normal-slip fault  
Left-normal-slip fault  
Right-reverse-slip fault  
Left-reverse-slip fault

Modified after Dennis.

Figure 7: Fault classification by slip sense.

## METHODS OF INVESTIGATION AND CORRELATION

### Methods of Investigation

The methods of investigation employed show basically one thing; the strike of the lineaments produced by the joints and or faults. The strike is the relatively straight line produced when the plane of a joint or fault intersects the surface of the earth. This straight line can then be termed as a lineament if it leaves a linear feature on the earth's surface.

The three methods of measurement used are satellite imagery, GQ's (geologic quadrangle maps) with previously mapped faulting, and direct measurement. Satellite imagery is a long process but is not hard to understand. The steps involved in a good satellite imagery study include several procedures. The first step is to obtain a satellite positive of the area in question. The positive is then "enhanced" through a camera and video edge enhancer (Figure 8). The image produced is then transmitted to a television monitor. From the television monitor a 35mm slide is taken of the image (Figure 9). After the slides are developed they can then be projected onto a standard 7.5-

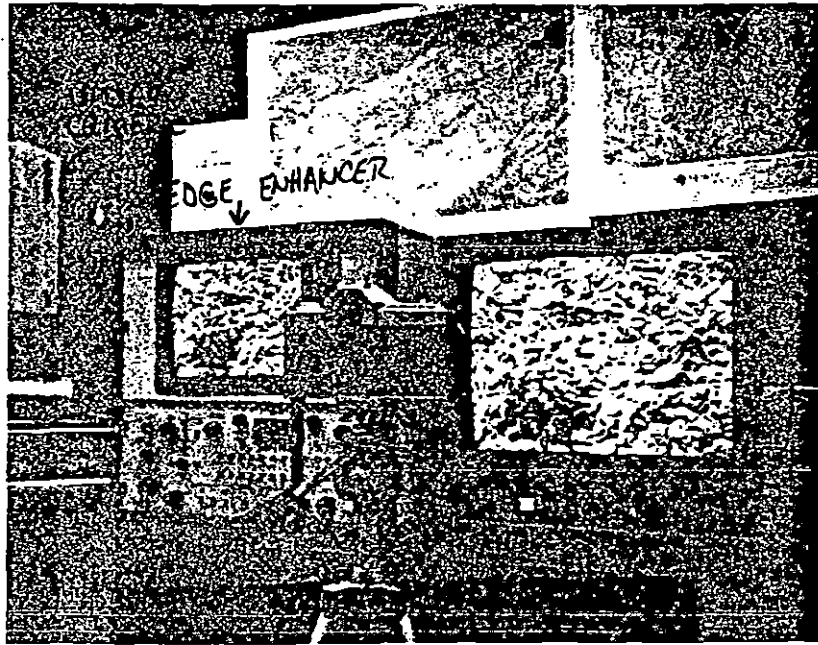


Figure 8: Picture showing video camera and edge enhancer.(Hylbert, 1984).

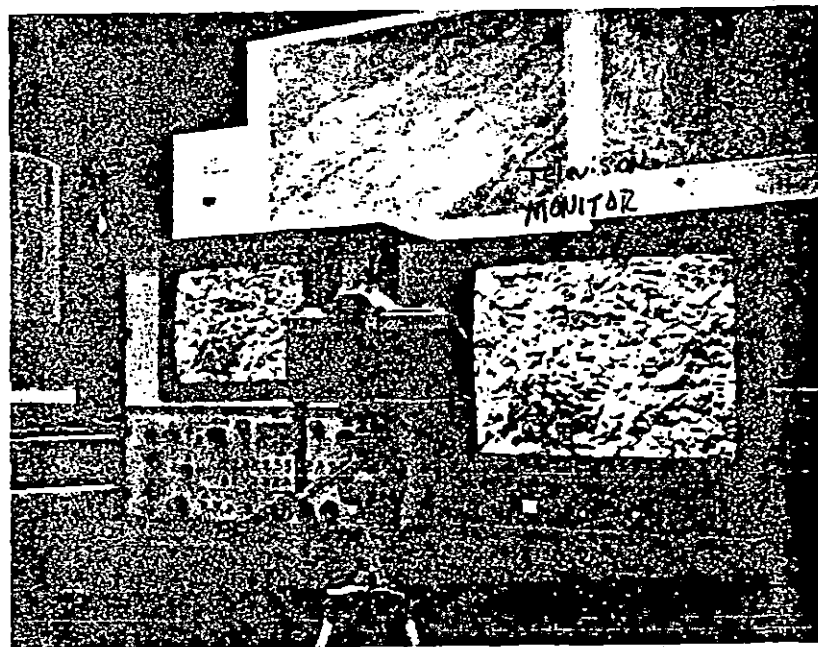


Figure 9: Picture showing television monitor and 35mm camera set-up(Hylbert, 1984).

minute topographic map at the same scale. When the projection and the map are properly aligned the combined image of the two appears to be a three dimensional picture (Figure 10). The lineaments do not show up well until the slide image is projected through a type of grating. The Ronchi grating is a thin plastic film with about 133 lines per inch. When the grating lines align with the lineaments of the satellite imagery, the linear trends lock in. With acetate film covering the map, trends can then be traced (Figures 10 & 11). After the lineaments are traced, a directional bearing can be taken with a protractor from the North arrow on the topographic map (Hylbert, 1984, p/30). A compilation of this data is necessary, but will be addressed later in the paper.

The second method of measurement involves the use of previously mapped faulting and jointing. While lineaments and joints are rarely put on GQ's, large faults are almost always marked. The significance of this is that with an exact location the structure is much more easily found. Once the location of this structure is known a field search of local jointing and faulting can be conducted. This leads to the last method of measurement.

The method of direct measurement is very important in determining the validity of the other

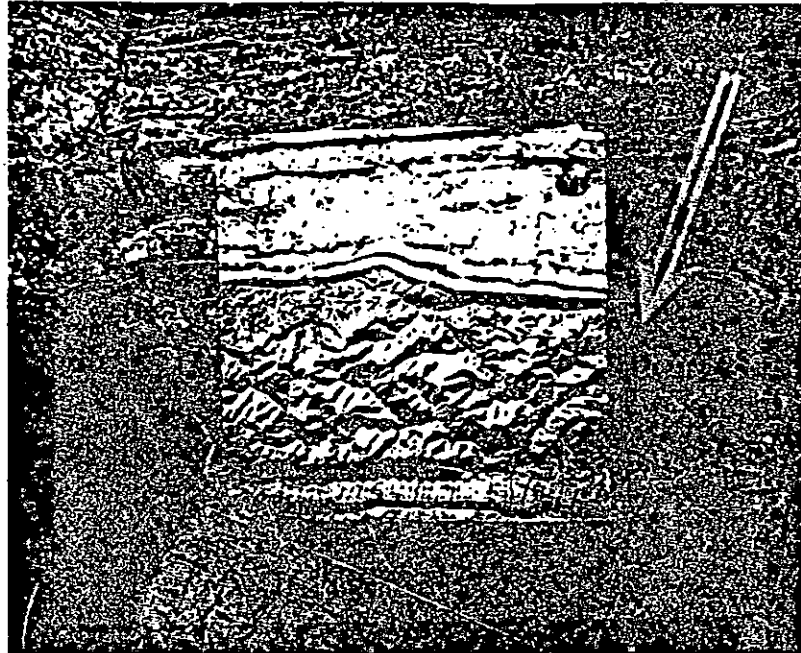


Figure 10: Three dimensional projection of satellite imagery onto topographic map (Hylbert, 1984)

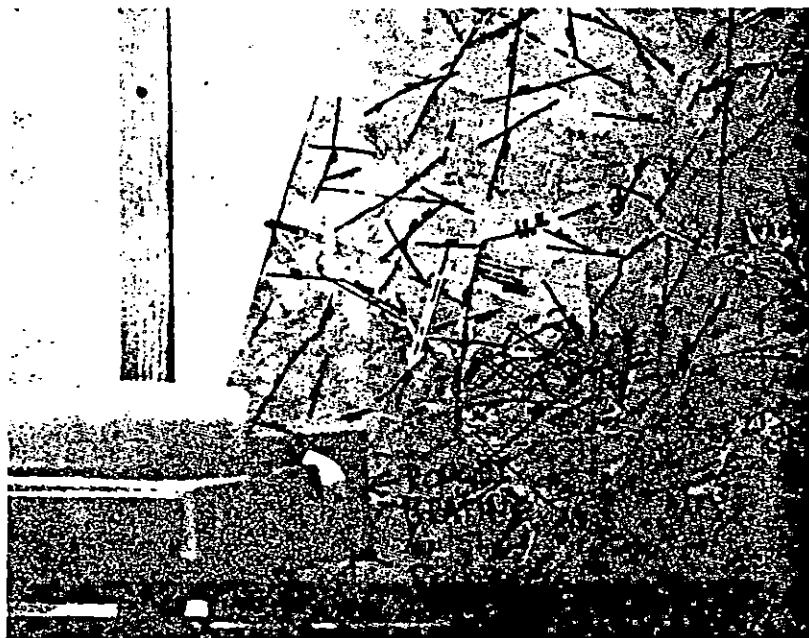


Figure 11: Picture showing Ronchi grating and the tracing of lineaments on a topographic map.

two methods. Direct measurement involves going out into the field and actually "taking" the strikes of structures such as faults and joints. This is accomplished by using the geologist's closest friend, the Brunton compass. To get good results several hundred measurements must be taken. Since this study is looking at a very broad view only a few measurements of this type were gathered. This information can be correlated with data from the satellite imagery and GQ's (Hylbert, 1993).

*Being a  
2nd level  
number, you  
need not have  
beginning &  
have page*

Methods of Correlation —

The method of correlation of this data employs the use of a rose diagram. A rose diagram is a sort of circular histogram that shows actual compass bearings(Figure 12). To use rose diagrams the various bearings must be divided into increments. For the purposes of this study 10 degree increments were used. This is a sort of way to average the directional trends. The rose diagrams used here were compiled by Rosy in the Rock Works software on a Macintosh LCII computer. By using software of this sort a great deal of time is saved because of its ability of data manipulation. The Rosy program supplies a great deal of statistical information but due to the complexity of this information, it was not used.

The importance of the rose diagram soon becomes apparent in this study. By entering the bearings of the satellite imagery into Rosy it is apparent that there are at least two distinct joint sets. The systematic joints of set one strike in the range of 60 degree  $\pm$  10 degree, while set two systematic joints strike nearly East-West(Figure 13). When compared to the previously marked faulting on the GQ's, the data was right on. The



Irvine-Paint Creek Fault(Figure 14) trends East-West with one joint set but each time the fault takes a turn it lines up with the other. The measured field data did not compare as well but this was probably due to the limited amount of data. The joints sets obtained from the rose diagram were still within about 10 degrees of each other(Figure 15). With more extensive data it can be assumed that the joint sets would have lined up more closely.

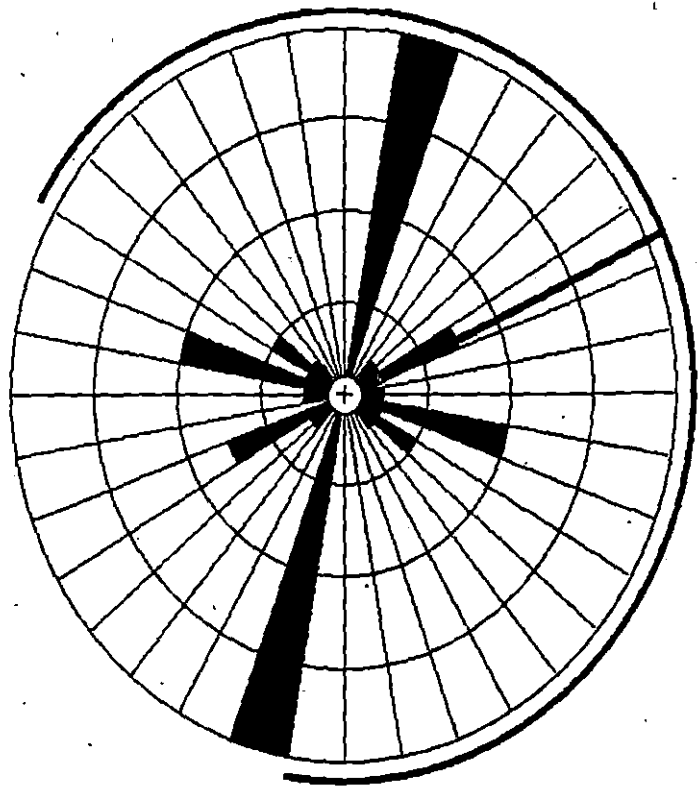


Figure 12: Rose diagram.

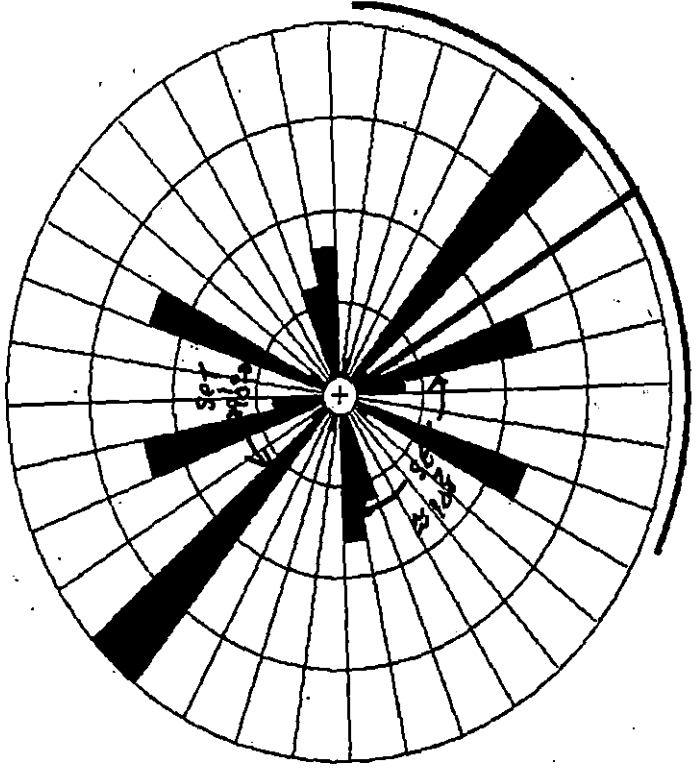


Figure 13: Rose diagram showing two distinct joint systems.

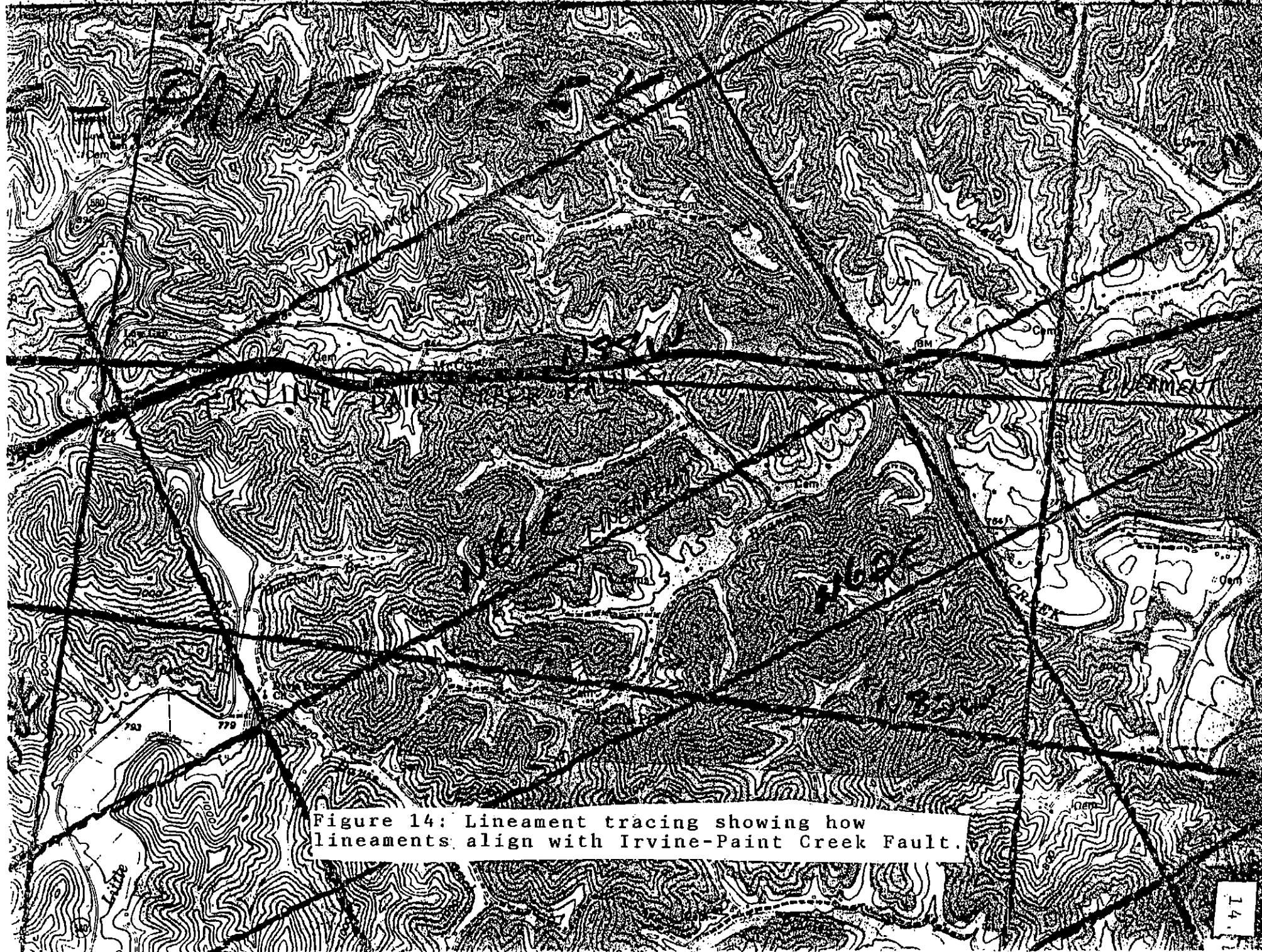


Figure 14: Lineament tracing showing how lineaments align with Irvine-Paint Creek Fault.

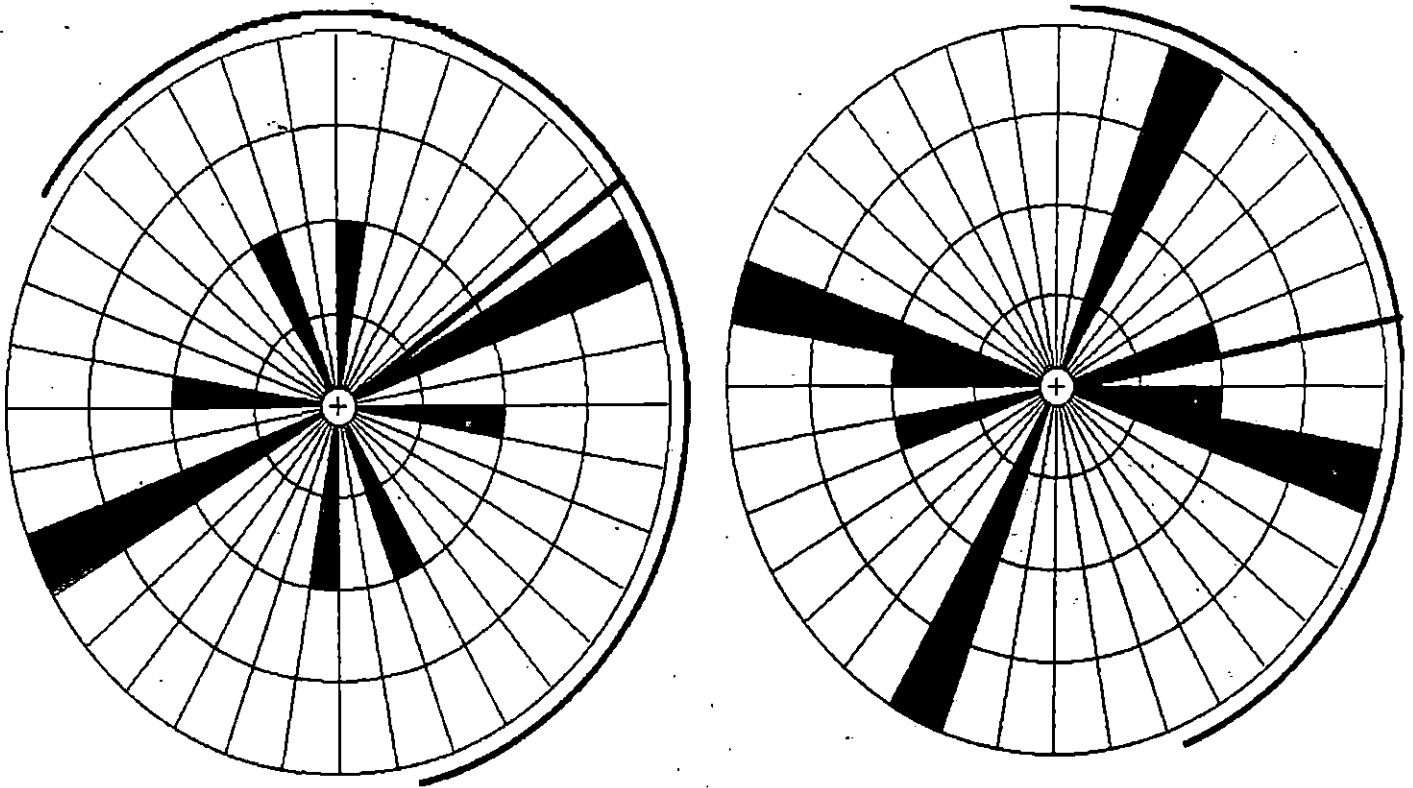


Figure 15: Rose diagrams showing comparison of satellite imagery data to field data.

## POSSIBLE CAUSES OF THE JOINTING AND FAULTING

## Possible Causes of Jointing

Determining the causes of jointing in the selected areas of Eastern Kentucky is almost beyond the scope of this research. A few observations were made that may help to start an explanation. The most obvious possible cause could be the Pine Mountain Thrust. Pine Mountain lies to the South of the research area (Figure 1). The strike of Pine Mountain appears to be nearly parallel with the systematic joints of joint system one. Since the age of the strata being dealt with is Pennsylvanian, it stands to reason that the jointing occurred at the earliest during the Permian. This is the period of time in which the Appalachian Orogeny occurred, and also Pine Mountain was formed.

There is no obvious cause to system two jointing. It is possible that they were formed at an earlier time than the Pennsylvanian rocks were deposited. If this is the case, then the jointing perpetuated up through the strata as it was formed. Another possible explanation is that the direction of the thrust changed and the system two joints

were also formed in the Permian just before the system one joints (Hylbert, 1993).

*2nd level  
found  
log on  
p. 17  
1st level*

### Possible Causes of Faulting

The possible causes of faulting in an area such as this are even more difficult to determine than the causes of jointing. The area being dealt with is relatively stable and not much tectonic activity has occurred. The structural significance of the area is minor (Jillson, 1920). A very hypothetical explanation follows.

When the thrust of Pine Mountain stopped, there was a release of pressure. The pressure was not great enough to cause reverse faulting but it was great enough to cause fracturing of the strata. When this pressure stopped there was a horizontal rebound of the earth's crust. The crust is such a massive object that it developed significant inertia during this rebound. The inertia from the rebound set up strain that pulled the strata apart at the joints (Figure 16). As was stated before this is a hypothetical explanation, but it does seem reasonable.

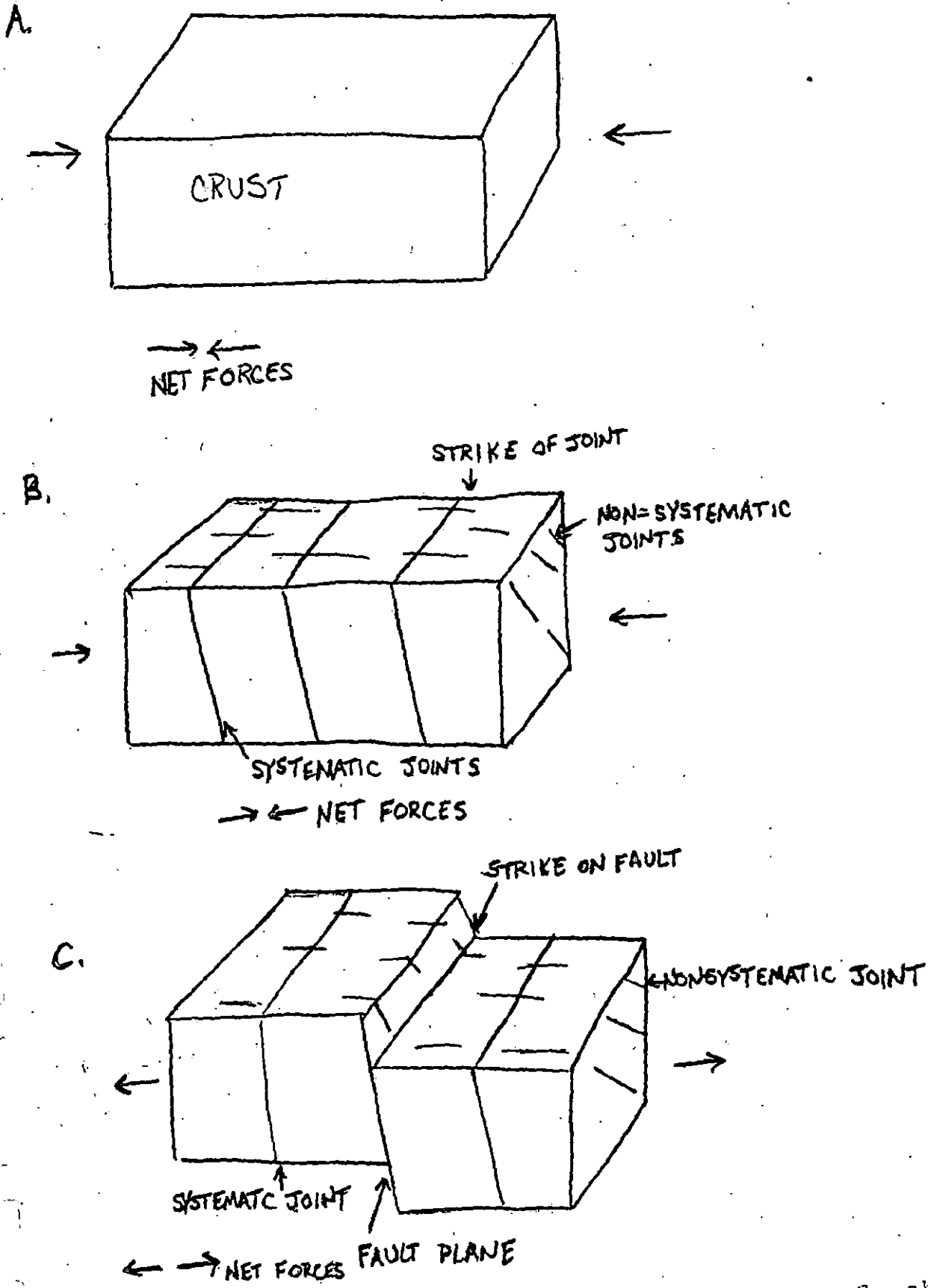


Figure 16: Sequence of events from A to C, showing what may have happened to cause jointing and faulting.



## ECONOMIC SIGNIFICANCE OF THIS STUDY

Studies of this type can be very important in coal mining and oil exploration. Coal mining probably benefits the most. Mine planning for under ground mines is a major area of concern, more specifically roof control. Mine planners could benefit by cutting across lineament that show up on satellite imagery and completely stay away from areas in which lineaments cross. This method of roof control is described <sup>in 1984</sup> in Geologic Structure and Mine Roof Falls in Selected Coal Beds Within Appalachia by D. K. Hylbert.

Oil exploration could also benefit from this type of study. If it could be proven that oil follows joint structures then wells could possibly be drilled with horizontal drilling rigs. If a fault or joint could be intercepted with this equipment the payoff would be great. This stands to reason because the area of study was once oil rich. Most of the oil was concentrated in dome structures (Hudnall<sup>x</sup> et al., 1924). If drainage is structure controlled, which it appears to be, the underground oil flow may also. The economic payoff

of an undertaking of this sort could be great  
(Reed, 1993).

CONCLUSION | *Int-level  
header should  
be on p. 22.*

The definitions of jointing are rigidly set, but their study and measurement is not. There are many techniques that have been and many more that will be developed to help us understand the processes that shape our world. Whether we study for economic gain or just an understanding we can only benefit.

## WORKS CITED

- Dennis, J.G., Structural Geology an Introduction, 1987, Wm. C. Brown Publishers, Dubuque, Iowa.
- Englund, K.J., and DeLaney, A.O., a, (1967), Geologic Map of the Ezel Quadrangle, (GQ-598) Kentucky, United States Geologic Survey, Washington, D.C.
- Englund, K.J., and DeLaney, A.O., b, (1966), Geologic Map of the Wrigley Quadrangle, (GQ-190) Kentucky, United States Geologic Survey, Washington, D.C.
- Englund, K.J., and DeLaney, A.O., c, (1966), Geologic Map of the Sandy Hook Quadrangle, (GQ-521) Kentucky, United States Geologic Survey, Washington, D.C.
- Englund, K.J., Huddle, J.W., and DeLaney, A.O., d, (1967), Geologic Map of the West Liberty Quadrangle, (GQ-599) Kentucky, United States Geologic Survey, Washington, D.C.
- Hudnall, J.S., and Browning I.B., (1923) Structural Geologic Map of the Paint Creek Uplift (Series VI). Kentucky Geologic Survey, Lexington, KY.
- Hylbert, D.K., Geologic Structure and Mine Roof Falls in Selected Coal Beds Within Appalachia, 1984, Morehead State University Printing Services, Morehead, KY.
- Hylbert, D.K., Personal Interview, Fall 1993.
- Jillson, W.R., Oil and Gas Resources of Kentucky, 1920, Kentucky Geologic Survey, Frankfort, KY.
- Outerbridge, W.F., e, (1963), Geologic Map of the Inez Quadrangle, (GQ-226) Kentucky, United States Geologic Survey, Washington, D.C.
- Outerbridge, W.F., f, (1967), Geologic Map of the Oil Springs Quadrangle, (GQ-586) Kentucky, United States Geologic Survey, Washington, D.C.
- Outerbridge, W.F., g, (1966), Geologic Map of the Paintsville Quadrangle, (GQ-495) Kentucky, United States Geologic Survey, Washington, D.C.
- Reed S.K., Personal Interview and Commits made during presentation of this paper. Fall 1993.

*Too many  
pages*

## JOINTING AND FAULTING IN SELECTED AREAS IN EASTERN KENTUCKY

Blair, Mark, A., Department of Physical Sciences,

Morehead State University, Morehead, KY 40351

The main fault system studied in Eastern Kentucky is that of the Irvine-Paint Creek Fault Zone. The faults in the area grade from medium to steeply dipping. Location and measurement of jointing and faulting is difficult due to lack of good outcrops and vegetation coverage. This is overcome in one of three ways. The first way is a lineament study. This procedure involves using satellite imagery and a video enhancer to "bring out" straight-line features in topography. These straight-line features are often the strikes of joints and faults. The second method is using geologic quadrangles with locations of previously mapped structures. While only large faults are mapped there is often associated faulting and jointing. The last method is a little random but often reveals well exposed joints and faults. It is merely driving along road cuts and outcrops looking for structures. The results of the latter of the two methods can be compared to the results of the first method to verify data. The data obtained is the strike of the features. This data is analyzed by means of a rose diagram. A rose diagram is a statistical plot that groups directional trends. The jointing and faulting in Eastern Kentucky studied occurred in Pennsylvanian age rock. From the data it was found that two distinct joint sets formed. One set lined up with the Pine Mountain Thrust that occurred in the Permian. The other set may have been caused earlier and the structure perpetuated up through the younger material as it was laid down. The faulting is probably a result of the release of pressure from discontinuance of the Appalachian Orogeny. The strain that was set up from this release may have formed the normal faults that we see today. The significance of this research is in the field of Economic Geology. These structures can help to predict areas prone to roof fall in underground mining and point us toward valuable and needed oil and gas deposits.

### MAJOR WORKS CITED

Hudnall, J.S., and Browning I.B., (1923) Structural Geologic Map of the Paint Creek Uplift (Series VI), Lexington, KY. Kentucky Geologic Survey.

Hylbert, D.K., Geologic Structure and Mine Roof Falls in Selected Coal Beds Within Appalachia, 1984, Publisher unknown.

Hylbert, D.K., Personal Interview, Fall 1993.

Jillson, W.R., Oil and Gas Resources of Kentucky, 1920, Kentucky Geologic Survey, Frankfort, KY.

MSU ARCHIVES

LIBRARY USE ONLY

